FINITE ELEMENT ANALYSIS OF BEAM WITH SMART MATERIALS

A thesis submitted in partial fulfilment of the requirement for the award of the degree of Bachelor of Technology in Civil Engineering

Submitted By:

PRATYUSH KUMAR PANDEY

(111CE0252)

Under the supervision of:

Prof. (Dr.) MANORANJAN BARIK

Department of Civil Engineering

NATIONAL INSTITUTE OF TECHNOLOGY ROURKELA

National Institute of Technology

Rourkela

CERTIFICATE

This is to certify that the thesis entitled, **"Finite Element Analysis of Beam with Smart Materials"** submitted by **Pratyush Kumar Pandey (111CE0252),** in partial fulfilment of the requirement for the degree of **Bachelor of Technology** in **Civil Engineering**, National Institute of Technology, Rourkela, is an authentic work carried out by him under my supervision.

To the best of my knowledge, the matter embodied in the thesis has not been submitted to any other university/institute for the award of any degree or diploma.

Date:

(Prof. Manoranjan Barik)
Dept of Civil Engineering
National Institute of Technology

Rourkela-769008

ACKNOWLEDGEMENTS

First of all, I would like to express my gratitude to my project guide **Prof. M.R. Barik.** I was a very fortunate undergrad to have such an enthusiastic guide who help me out through the whole process of the project work. I could not find words to mouth my gratitude. The immense help and support received from him inspired me to learn and to be an asset to the vast arena of civil engineering in the Indian scenario during this project. This was really a great experience for me to work with him.

I also thank **Prof. S. K. Sarangi**, **Director, NIT Rourkela** and **Prof. S. K. Sahu**, Head of the **Civil Engineering Department, NIT Rourkela**, for furnishing me with the required facilities to carry out my research work.

I would also like to thank all the faculty members and staffs of civil engineering department for their assistance in my research work, as well as in my undergraduate studies.

I am also thankful to my batch mates who directly or indirectly have helped me a lot in completing my research work.

I would also like to thank my parents, who have supported me a lot and without whose blessings, this project would not have been possible.

At last, I would once again like to thank Prof M.R. Barik, without whose guidance I could not have completed my project.

PRATYUSH KUMAR PANDEY

ABSTRACT

Impedance-based structural health-monitoring techniques are developed by utilizing a number of smart material technologies and represent a new non-destructive evaluation (NDE) method. The basic concept of this approach is monitoring the variations in mechanical impedance of the structure resulted by the presence of damage. Since it is very difficult to measure the structural mechanical-impedance, the new impedance methods utilize the electromechanical coupling properties of piezoelectric materials.

The impedance-based structural health monitoring is done by using piezoelectric patches which are bonded to the host structure that act as both sensors and actuators on the system. When a PZT comes under a change in environment, it produces an electric charge. Conversely when an electric field is applied the PZT undergoes a mechanical strain. A sinusoidal voltage is used for the excitation of the PZT patch. As the patch is surface bonded to the host structure, the structure deforms along with it and gives a local dynamic response to the vibration. That response is then transmitted back from the PZT patch as an electrical response. The electrical response is then analysed where damage is shown as a phase shift or magnitude change in the impedance.

In this project finite element simulation of the interaction between a PZT patch and a structure utilizing the electromechanical impedance (EMI) technique is studied. Simulation of the host structure with a piezoelectric patch at a high frequency range (up to 1000 kHz) using ANSYS version 13, was successfully performed. Advantages over the traditional FEA based impedance model and the impedance based analytical models include higher accuracy, direct acquisition of electrical admittance/impedance. This study proves that the FEM could emerge as an excellent alternative to structural health monitoring by visual inspection method.

TABLE OF CONTENTS

LIST OF FIGURES

LIST OF TABLES

CHAPTER 1

INTRODUCTION

1.1 Introduction

Structural health monitoring is the continuous measurement of the loading environment and the critical responses of a system. SHM is typically used to evaluate performance, symptoms of operational incidents, and anomalies due to damage as well as health during and after an extreme event. Health monitoring has received considerable attention in civil engineering in the recent times. Although health monitoring is a new concept in the manufacturing, automotive and aerospace industries, there are a number of challenges for effective applications on civil infrastructure systems. Health monitoring offers great promise for civil infrastructure implementations. Although it is still mainly a research area in civil infrastructure application, it would be possible to develop successful real-life health monitoring systems if all components of a complete health monitoring design are recognized and integrated.

The main requirement of a successful health monitoring design is the recognition and integration of several components. The first component is the identification of health and performance metric which is a fundamental knowledge needed and it should govern the technology involved.

Development, evaluation and utilization of the new techniques are important but they must be considered along with our "health" and "performance" expectations of the structure. Yao and Natke [18] defined the term damage as a deficiency or deterioration in the strength of the structure, caused by external loading or environmental conditions or human errors. So far visual inspection has been the most common tool to identify the external signs of damage in buildings, bridges and industrial structures. These inspections are made by trained personnel. Once gross assessment of the damage location is made, localized techniques such as acoustic, ultrasonic, radiography, eddy currents, thermal, or magnetic field can be used for a more refined assessment of the damage location and severity. If necessary, test samples may be extracted from the structure and examined in the laboratory. One essential requirement of this approach is the accessibility of the location to be inspected. In many cases critical parts of the structure may not be accessible or may need removal of finishes. This procedure of health monitoring can therefore be very tedious and expensive. Also, the reliability of the visual inspection is dependent, to a large extent, on the experience of the inspector. Over the last two decades number of studies have been reported which strive to replace the visual inspection by some automated method, which can enable more reliable and quicker assessment of the health of the structure. Smart structures is found to be the alternative to the visual inspection methods from last two decades, because of their inherent 'smartness', the smart materials exhibit high sensitivity to any changes in the environment.

1.2 Need for structural health monitoring

Appropriate maintenance prolongs the life span of a structure and can be used to prevent catastrophic failure. Higher operational loads, greater complexity of design and longer life time periods imposed to civil structures, make it increasingly important to monitor the health of these structures. Economy of a country depends on the transportation infrastructures like bridges, rails, roads etc., any structural failure of buildings, bridges and roads causes severe damage to the life and economy of the nation. Every government is spending many crore of rupees every year for the rehabilitation and maintenance of large civil engineering structures.

Failure of civil infrastructure to perform may affect the gross domestic production of the country.

1.3 Methods of health monitoring

There are basically two methods of health monitoring. These are

1. Visual inspection

2. Automated health monitoring

In visual inspection method inspections are made by trained personnel. Once gross assessment of the damage location is made, localized techniques such as acoustic, ultrasonic, radiography, eddy currents, thermal, or magnetic field can be used for a more refined assessment of the damage location and severity. If necessary, test samples may be extracted from the structure and examined in the laboratory.

In automated health monitoring the detection of damage is done by using various smart materials which have the characteristics that enables them to react to any changes in their loading environment in a predetermined manner. It means that one of their properties can be altered by an external condition, such as temperature, pressure or electricity. This change in property is reversible and hence can be repeated many times.

1.4 Need for an automated health monitoring system

Even though visual inspection is the most common technique at present, it is very tedious, and needs experienced people. Over the last two decades, many researchers have tried to find the alternative solution for visual inspection. One essential requirement of this approach is the accessibility of the location to be inspected. In many cases critical parts of the structure may not be accessible or may need removal of finishes. This procedure of health monitoring can therefore be very tedious and expensive. Also, the reliability of the visual inspection is dependent, to a large extent, on the experience of the inspector. These facts underlining the importance of an automated health monitoring system, which can not only prevent an incipient damage including collapse, but also can make an assessment of structural health, as and when desired, at a short notice. These automated systems hold the promise for improving the performance of the structure with an excellent benefit/cost ratio, keeping in view the long term benefits.

1.5 Techniques of structural health monitoring

There are mainly two types of structural health monitoring system.

1. Wired techniques
2. Wireless techniques

WIRED TECHNIQUES

When sensors are physically in contact with the structure/body on which we are going to investigate for damage detection, then such kind of technique is referred as wired techniques. Wired techniques are widely used in present situation and uses smart sensors, fiber optics sensors, etc. Sensors and sensors characteristics depends on the location, Material, and methods applying to detect the flaws or faults. Generally Vibration based method, Impedance based method, Data fusion method, and inverse methods are used in wired techniques. These techniques are discussed below:

Impedance-Based Structural Health Monitoring Techniques

Electrical impedance is the measure of the opposition that a circuit presents to the passage of a current when a voltage is applied. With the help of resistance on current flow measured by the computer system installed with related software gives electric signature through which we can find out risk zone.

Impedance based structural Health Monitoring can be done by different techniques like by Analogue and digital formats using PZT patches, Frequency variation approaches. In the EMI based health-monitoring technique, the detection of damage is done by using a scalar damage metric, which is defined as the sum of the squared differences of the real impedance changes at every frequency step. The damage metric simplifies the analysis of impedance variations and gives a summary of the information obtained from the impedance response curves.

In SHM using PZT patch, piezoelectric transducer acting in the ‘‘direct’’ manner produces an electrical charge when it comes under mechanical stress. Conversely, the transducer undergoes a mechanical strain when an electrical field is applied. The method to be adopted with the EMI based SHM uses both the direct and converse versions of the piezoelectric effect to get the conductance signature of the structure. When a PZT patch attached to a host structure is excited by an alternating electric field, the PZT wafer and the structure undergoes a small deformation. Since high frequency is used for the excitation, the dynamic response of the structure reflects only a very local area to the sensor. The response of that local area is then transferred back to the PZT wafer in the form of an electrical response.

The electromechanical modelling that describes the process is presented in Figure 1.1. The PZT is normally surface bonded to the host structure by an adhesive to ensure good mechanical interaction.

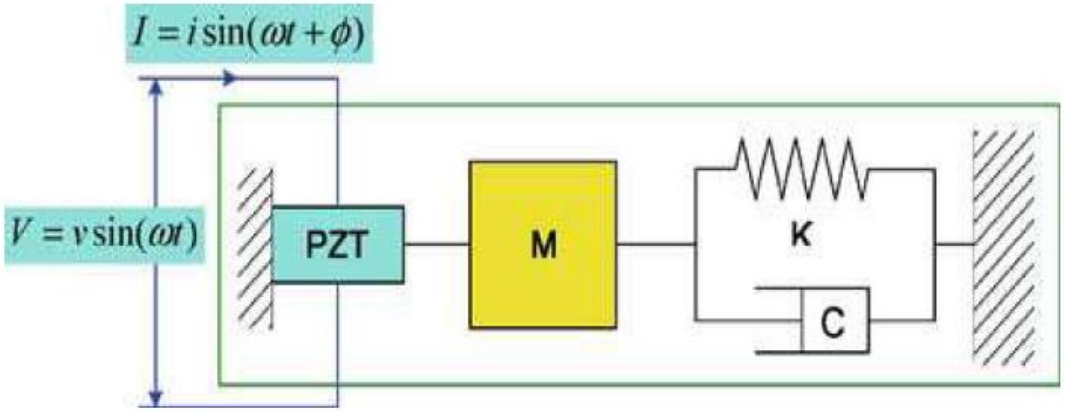

Figure 1.1: Electro-Mechanical Impedance System

Data Fusion Technique

Data fusion techniques can combine data from multiple sources and related information from associated databases to achieve higher accuracy and more specific inferences than by the use of a single source alone. When structure gets damaged due to natural disaster, at that moment structural component also get damaged due to the vibration and other effects. Hence to detect exact and accurate zone of damage, data fusion technique is used.

Vibration Control Technique

Stochastic Subspace-Based Fault Detection Method (SSFD) used in France, Inverse Technique, Time domain method, Frequency domain method, these techniques are used in vibration control technique. According to Rytter, there are 4 levels on the damage assessment scale, where the information about the damage is increased from step to step: Level I: Damage detection; Level II: Damage localization; Level III: Damage quantification and Level IV: Prognosis of remaining service life [4]. This concept comprises six modules those included data sensing, Acquisition, processing, management and finally monitoring.

WIRELESS TECHNIQUE

Spatially distributed autonomous sensors to monitor physical information without physically in contact with particular object, but by the help of data received from it, can analyse several important features. Structural health monitoring using wireless technique invents presently and it requires a High resolution images or data. Wireless sensors can be used to detect the defect within the buildings, bridges, embankments, and tunnel. Basically in SHM it is applicable to simulate load carrying capacity, fatigue resistance, Vibration control for the structure and finally for crack detection. Wireless SHM is important mainly for large structure where wired techniques spend more time as well as fund, but it performs a whole detection at once hence time saving as well as fund too. Generally it is most useful on bridge structure. Active and passive sensors are used to capture data and are evaluated with the help of special computer system along with software like Arc GIS. In the conventional SHM system, the expensive cost for purchase and installation of the SHM system components, such as sensors, data loggers, computers, and connecting cables, is a big obstruction. To guarantee that measurement data are

reliably collected, SHM systems generally employ coaxial wires for communication between sensors and the repository. However, the installation of coaxial wires in structures is generally very expensive and labour-intensive [3].

CHAPTER 2

REVIEW OF LITERATURE

2.1 Literature Review

Daniel [13] applied a promising SHM method on structures which is EMI based health monitoring. Although impedance-based SHM does not typically use an analytical model for basic damage identification, a model is necessary for more advanced features of SHM, such as damage prognosis, and to evaluate system parameters when installing on various structures. He developed a model based on circuit analysis of the previously proposed low-cost circuit for impedance-based SHM in combination with spectral elements.

Victor [7] reviewed the state of the art in structural health monitoring with piezoelectric wafer active sensors and highlighted the limitations of the current approaches which are predominantly experimental. Subsequently, he examined the needs for developing a predictive modelling methodology that would allow to perform extensive parameter studies to determine the sensing method's sensitivity to damage and insensitivity to confounding factors such as environmental changes, vibrations, and structural manufacturing variability. The thesis is made such that a predictive methodology should be multi-scale and multi-domain, thus encompassing the modelling of structure, sensors, electronics, and power management. He also gave a few examples of preliminary work on such a structural sensing predictive methodology.

Yang et al. [16] presented this paper for the finite element simulation of the interaction between a PZT patch and a host structure, including the bonding layer, utilizing the EMI technique with varying temperature. He performed the simulation of the PZT–structure interaction at the high frequency range (up to 1000 kHz) using FEM software, ANSYS version 8.1.

Yang et al. [15] implemented Piezo-electric ceramic Lead Zirconate Titanate (PZT) based EMI technique for SHM to various engineering systems. In this paper he used the structural mechanical impedance extracted from the PZT electromechanical conductance signature as the damage indicator. A comparison study on the sensitivity of the electromechanical admittance and the structural mechanical impedance to the damages in a concrete structure is conducted. Results show that the structural mechanical impedance is more sensitive to the damage than the electromechanical admittance thus a better indicator for damage detection.

Yang et al. [17] applied Piezo-electric transducers, working on the EMI technique for health monitoring in aerospace, civil and mechanical engineering. The piezoelectric transducers are usually bonded on the surface of the structure and subjected to excitation so as to interrogate the structure at the desired frequency range. The interrogation resulted in the conductance signatures which can be used to estimate the structural health or integrity according to the changes of the signatures.

Duan et al. [5] reviewed the implementation of piezoelectric transducers in health monitoring. The analysis of plain piezoelectric sensors and actuators and interdigital transducer and their applications in beam, plate and pipe structures for damage detection are reviewed in detail.

Zhang et al. [19] studied the EMI technique for health monitoring. In this paper, he presented an impedance model for predicting the electromechanical impedance of a cracked beam. He analysed a coupled system of a cracked Timoshenko beam with a pair of PZT patches surface bonded to the top and bottom of the beam. He introduced the shear lag model to describe the load transfer between the piezoelectric patches and the cracked beam. He simulated the beam crack as a massless torsional spring.

Chhabra et al. [2] dealt with the Active Vibration control of structures with piezoelectric patches bonded on top and bottom surfaces of the beam. The patches are located at the different positions to determine the better control effect. The study is demonstrated through simulation in MATLAB.

Peng [14] studied the mechanical properties of steel fiber reinforced concrete crack for SHM. Since working environment is very harsh, the steel fiber reinforced concrete is prone to crack and a small crack on beam may result in severe damage. Hence, it is important to examine the mechanical properties of steel fiber reinforced concrete crack to detect early crack semiotics. He inspected the mechanical characteristics of steel fiber reinforced concrete crack by experimental tests on four specimens. He considered the effect of the loading position in the tests.

Hong et al. [8] modelled a strain-based load identification for beam structures subjected to multiple loads. In his model, he measured the contribution of each load to the strains by strain sensors. In this paper, the longitudinal strains measured from multiplexed fiber Bragg grating (FBG) strain sensors are utilized in the load identification.

Parameswaran et al. [12] studied the response of the mechanical systems from undesirable vibrations during their operations. Their occurrence is uncontrollable as it depends on various factors. However, for efficient operation of the system, these vibrations have to be controlled within the specified limits. Light weight, rapid and multi-mode control of the vibrating structure is possible by the use of piezoelectric sensors and actuators and feedback control algorithms. In this paper, direct output feedback based active vibration control has been implemented on a cantilever beam using Lead Zirconate-Titanate (PZT) sensors and actuators. Three PZT patches were used, one as the sensor, one as the exciter providing the forced vibrations and the third acting as the actuator that provides an equal but opposite phase vibration/force signal to that of sensed so as to damp out the vibrations. The designed algorithm is implemented on Lab VIEW 2010 on Windows 7 Platform.

Hu et al. [9] studied the application of Piezo-electric lead zirconate titanate (PZT) as a new smart material for health monitoring. To study the damage detection properties of PZT on concrete slabs, simply supported RCC slabs with PZT patches surface bonded to the host structure were chosen as the objective of the research and the electromechanical impedance technique was adopted for research. Five different kinds of damage were analysed to test the impedance values at different frequency bands.

2.2 Objective and Scope of Study

The objective of this project is to develop methodologies for finite element analysis of smart structures. In specific, the project attempts to obtain numerical simulation results for health monitoring of Reinforced concrete (RC) beam, using finite element analysis. Purpose of Numerical simulation is to avoid tedious experimental work of subjecting the structure to numerous fractures in future research, thereby saving time and money in future research.

Although the results of finite element analysis of beam with smart materials are already available in the literature work and the analysis of these beams have been done by various methods like finite element analysis, FSDT, ANSYS, and several other analytical and semi analytical method few studies have been done on the problem of Structural Health Monitoring(SHM) with PZT and I believe it to be newly considered theory that could be used as means of comparison and also for use in applications . This would also enhance my knowledge on the topic.

CHAPTER 3

THEORETICAL FORMULATION

3.1 Introduction

Many finite element models on PZT–structure interaction have been proposed in the last three decades. Lalande [10] provided a review into the finite element approaches for the simulation of interaction of the PZT patch with the host structure. He broadly classified them into three different categories, namely direct formulation of elements for specific application, utilization of a thermoelastic analogy, and the use of commercially available FE analysis (FEA) codes incorporated with piezoelectric element formulation. Fairweather [6] developed an FEA based impedance model for the prediction of structural response to induced strain actuation. The model utilized the FEM to determine the host structure's impedance.

3.2 One Dimensional Analytical Model for a Freely Suspended PZT Patch

An analytical model of a freely suspended PZT patch can be obtained by setting the mechanical impedance of the host structure to zero in the impedance based electromechanical coupling equations.

For the 1D free PZT patch model, the impedance based electromechanical coupling equation proposed by Liang *et al. [11]* can be reduced to (when $Z = 0$)

$$\bar{Y} = 2\omega i \frac{wl}{h}\left[\overline{\varepsilon_{33}^{T}} + d_{31}^{2}\overline{Y_{11}^{E}}\left(\left(\frac{\tan kl}{kl}\right) - 1\right)\right]$$

where ω = angular frequency of the driving voltage
i = imaginary number
w = *width of the PZT patch*
l = *half-length of the PZT patch*
h = thickness of the PZT patch
ε_{33}^{T} = complex dielectric permittivity
d_{31} = piezoelectric strain coefficient
$\overline{Y_{11}^{E}}$ = complex Young's modulus
K = wavenumber.

Rearranging the terms and expressing them in terms of real and imaginary components,

$$\bar{Y} = \left\{-4\pi f \frac{w}{h}\left[d_{31}^{2}Y_{11}^{E}(t + \eta(r-1) - \delta\varepsilon_{33}^{T})\right]\right\} + i\left\{4\pi f \frac{wl}{h}\left[\varepsilon_{33}^{T} + d_{31}^{2}Y_{11}^{E}(r - \eta t - 1)\right]\right\}$$

where *f is* the frequency,$r + ti = \frac{\tan kl}{kl}$, $\overline{Y_{11}^{E}} = Y_{11}^{E} + (1 + \eta i)$, $\overline{\varepsilon_{33}^{T}} = \varepsilon_{33}^{T}(1 - \delta i)$ with δ and η indicating the electrical loss factor and mechanical loss factor respectively.

3.3 Two Dimensional Analytical Model for a Freely Suspended PZT Patch

For 2D modelling of a freely suspended PZT based on cross impedance using the equation proposed by Zhou *et al. [20]*, the PZT could be modelled by setting all four terms related to the structural mechanical impedance to zero. The equation can thus be reduced to

$$\bar{Y} = 4i\omega\frac{wl}{h}\left[\overline{\varepsilon_{33}^{T}} - \frac{2d_{31}^{2}\overline{Y^{E}}}{(1-\nu)} + \frac{d_{31}^{2}\overline{Y^{E}}}{(1-\nu)} \times \left\{\frac{\sin\kappa l}{l} \middle| \frac{\sin\kappa w}{w}\right\}\begin{bmatrix}\kappa\cos\kappa l & 0\\ 0 & \kappa\cos\kappa w\end{bmatrix}^{-1}\right]$$

where *v* is the Poisson ratio. Again, rearranging and expressing in complex notation,

$$\bar{Y} = 8\pi f\frac{wl}{h}\left\{\left[\varepsilon_{33}^{T}\delta - \frac{d_{31}^{2}Y^{E}}{(1-\upsilon)}\left(t + T + \eta(r + R - 2)\right)\right] + i\left[\varepsilon_{33}^{T} + \frac{d_{31}^{2}Y^{E}}{(1-\upsilon)}[r + R - \eta(t + T) - 2]\right]\right\}$$

where $R + T\,\mathrm{i} = \frac{\tan kw}{kw}$.

Similarly, setting the effective structural impedance to zero in the 2D effective impedance modelling equation [1] yields

$$\bar{Y} = 4wi\frac{l^{2}}{h}\left[\overline{\varepsilon_{33}^{T}} + \frac{2d_{31}^{2}\overline{Y^{E}}}{(1-\nu)}\left(\frac{\tan kl}{kl} - 1\right)\right]$$

Again, rearranging and expressing in complex notation,

$$\bar{Y} = 8\pi f\frac{l^{2}}{h}\{[\delta\varepsilon_{33}^{T} - N(t + \eta r - \eta)] + i[\varepsilon_{33}^{T} + N(r - \eta t - 1)]\}$$

where $N = \frac{2d_{31}^{2}Y^{E}}{(1-\nu)}$.

CHAPTER 4

METHODOLOGY

4.1 ANSYS

For modelling and analysis of beam with PZT patch, Ansys 13.0 version is to be used which is based on Finite Element Method (FEM).

ANSYS Mechanical software is a comprehensive FEA analysis tool for structural analysis, including linear, nonlinear and dynamic studies. The engineering simulation product provides a complete set of elements behaviour, material models and equation solvers for a wide range of mechanical design problems. In addition, ANSYS Mechanical offers thermal analysis and coupled-physics capabilities involving acoustic, piezoelectric, thermal–structural and thermo-electric analysis.

FEA analysis (finite element) tools from ANSYS provide the ability to simulate every structural aspect of a product:

- Linear static analysis that simply provides stresses or deformations
- Modal analysis that determines vibration characteristics
- Advanced transient nonlinear phenomena involving dynamic effects and complex behaviours
- Harmonic response analysis are used to determine the steady-state response of a linear structure to loads that vary sinusoidal (harmonically) with time, thus enabling you to verify whether or not your designs will successfully overcome resonance, fatigue, and other harmful effects of forced vibration.

Ansys mechanical APDL is used for this purpose. APDL stands for ANSYS Parametric Design Language, a scripting language that you can use to automate common tasks or even build your model in terms of parameters (variables).

APDL is the foundation for sophisticated features such as design optimization and adaptive meshing, it also offers many conveniences that you can use in your day-to-day analysis.

SOLID5:

SOLID5 has a 3-D magnetic, thermal, electric, piezoelectric, and structural field capability with limited coupling between the fields. The element has eight nodes with up to six degrees of freedom at each node. Scalar potential formulations (reduced RSP, difference DSP, or general GSP) are available for modeling magneto-static fields in a static analysis. When used in structural and piezoelectric analysis, SOLID5 has large deflection and stress stiffening capabilities.

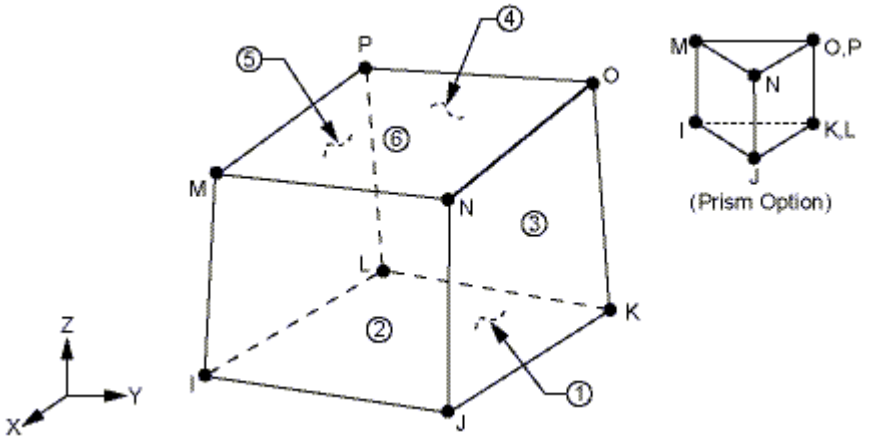

Figure 4.1: Geometry of Solid5 Element

Solid226:

SOLID226 has the following capabilities:

- Structural-Thermal
- Piezoresistive
- Electroelastic
- Piezoelectric
- Thermal-Electric
- Structural-Thermoelectric
- Thermal-Piezoelectric

The element has twenty nodes with up to five degrees of freedom per node. Structural capabilities include elasticity, plasticity, viscoelasticity, viscoplasticity, creep, large strain, large deflection, stress stiffening effects, and prestress effects. Thermoelectric capabilities include Seebeck, Peltier, and Thomson effects, as well as Joule heating. In addition to thermal expansion, structural-thermal capabilities include the piezocaloric effect in dynamic analyses. The Coriolis Effect is available for analysis with structural degrees of freedom.

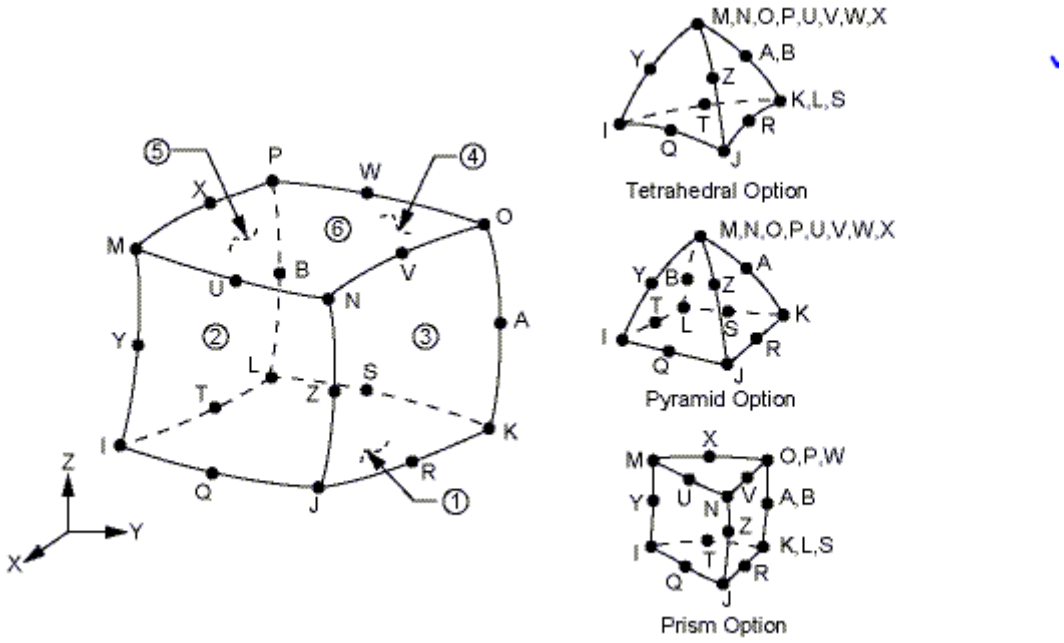

Figure 4.2: Geometry of Solid226 Element

4.2 Procedural Steps for Modelling

MODELLING OF FREELY SUSPENDED PZT PATCH:

The procedural steps required for modelling of freely suspended PZT patch using ANSYS 13.0 version are as follows:

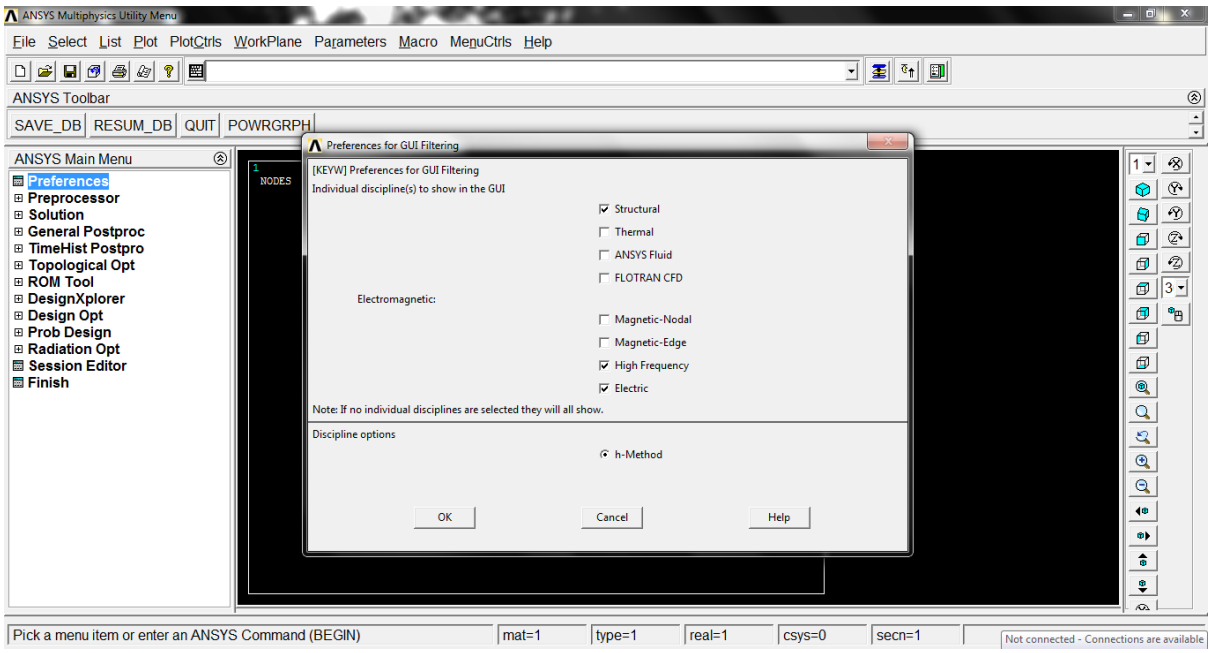

1. Preferences →Structural, Electric and High Frequency →Ok

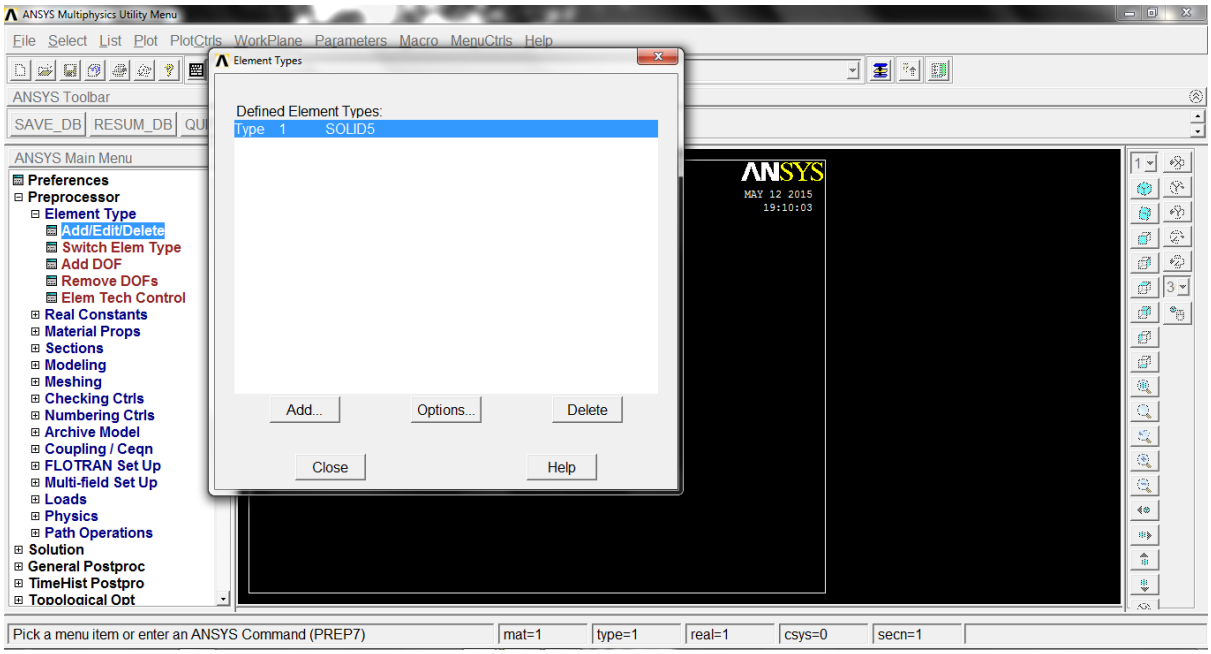

2. Preprocessor →Element type →Add →Coupled Field →Scalar Brick 5 →Ok

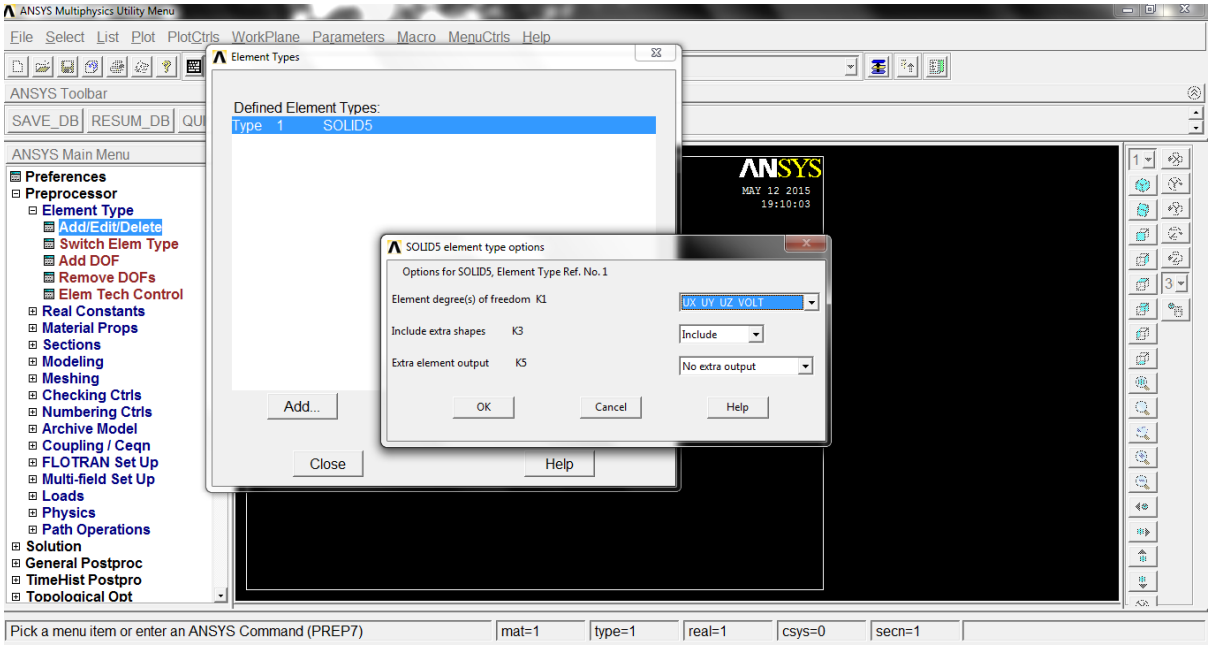

3. Options →Choose UX UY UZ VOLT from the first list →Ok

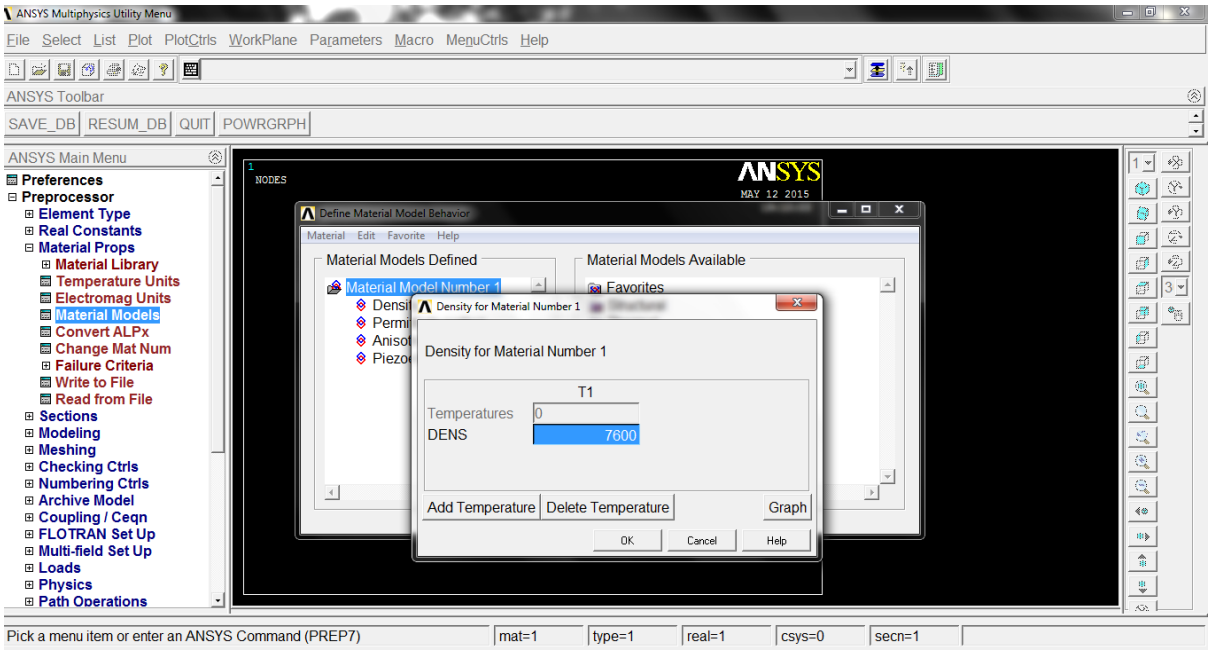

4. Material Properties →Material Models →Structural →Density →Enter the value →Ok

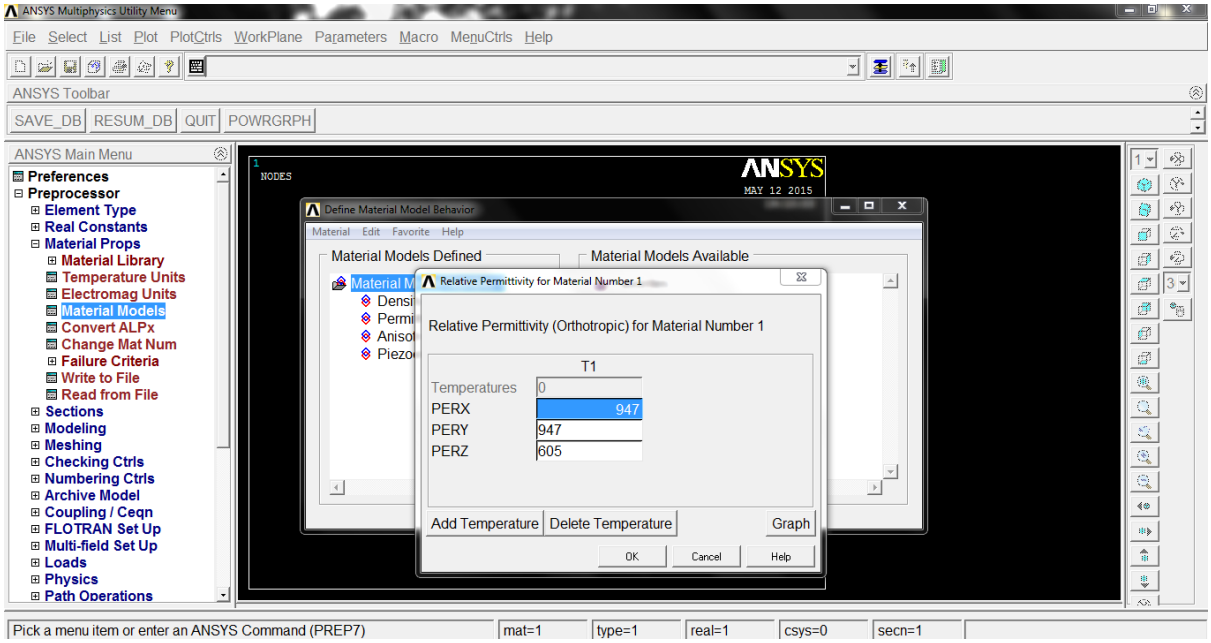

5. Electromagnetics →Relative Permittivity →Orthotropic →Enter the value →Ok

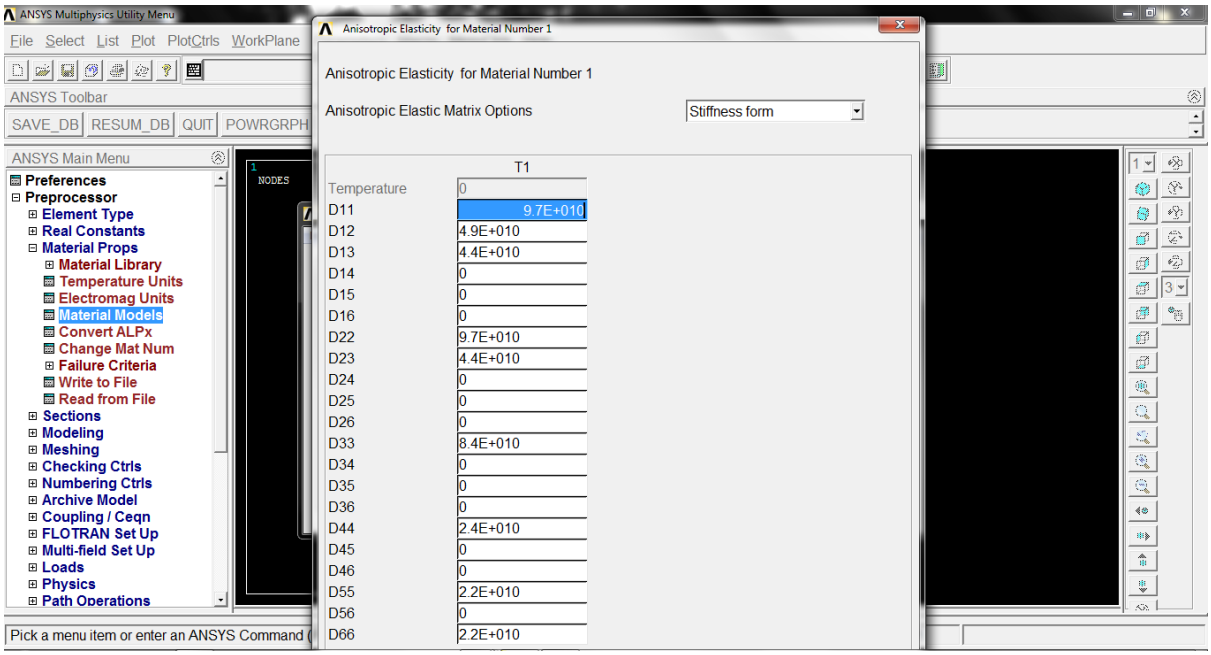

6. Structural →Linear →Elastic →Anisotropic →Enter the value →Ok

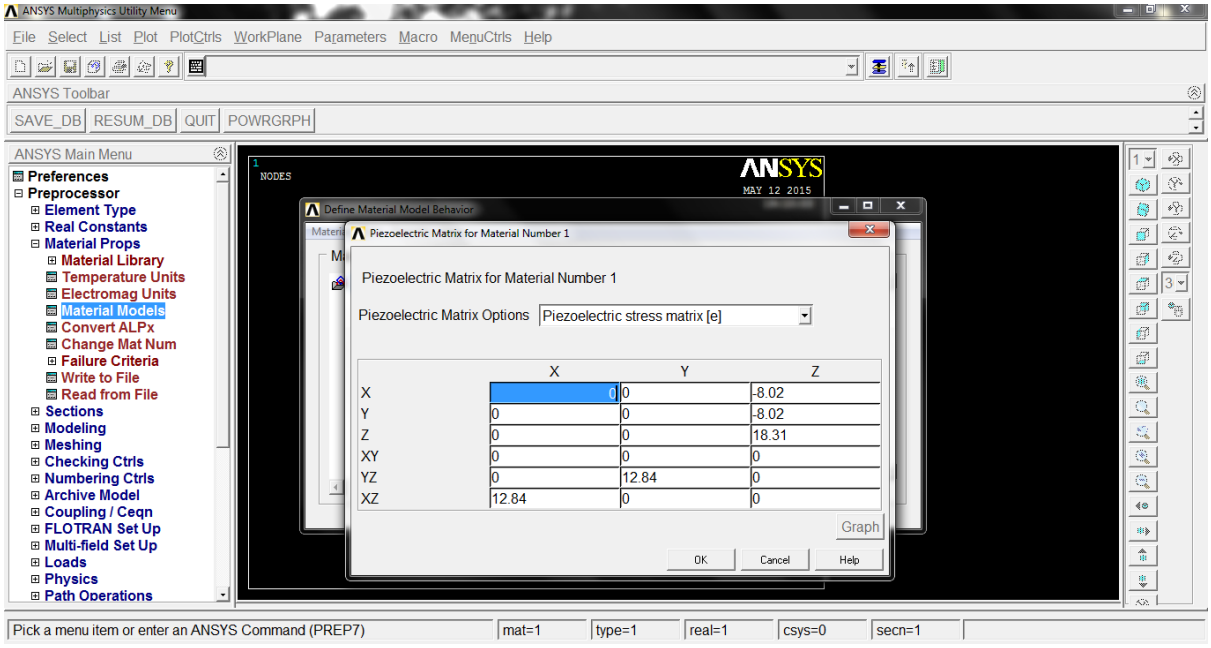

7. Piezoelectrics →Piezoelectric Matrix →Enter the value →Ok

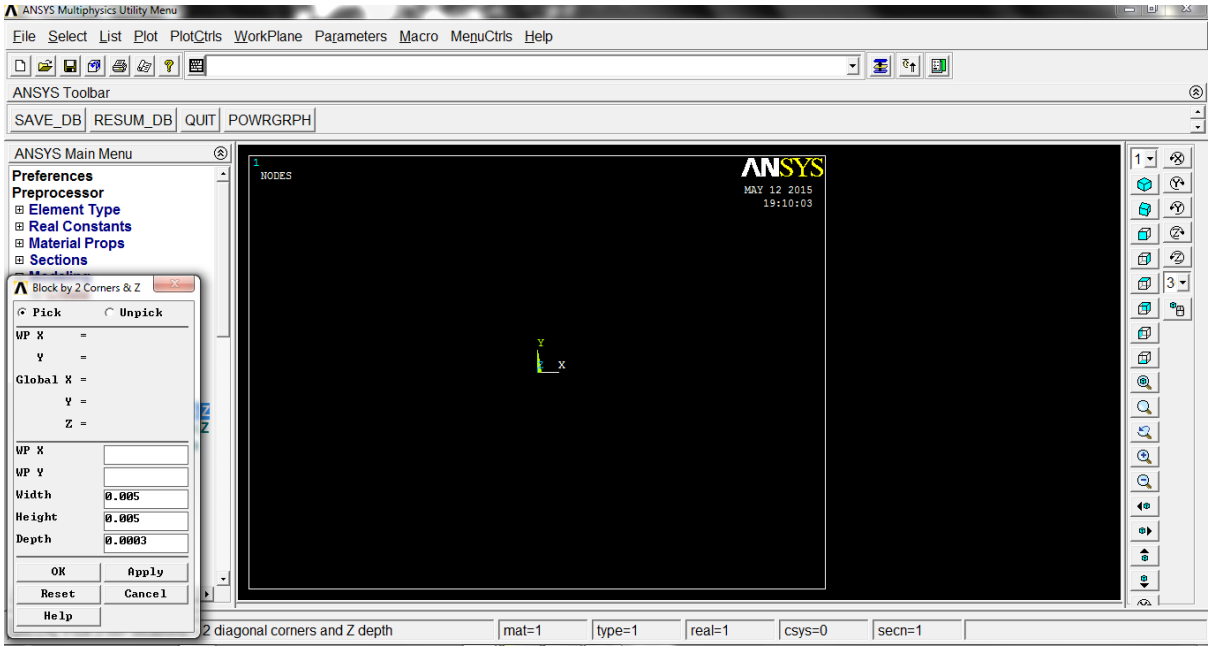

8. Modeling →Create →Volumes →Block →By 2 corners & Z →Enter the value →Ok

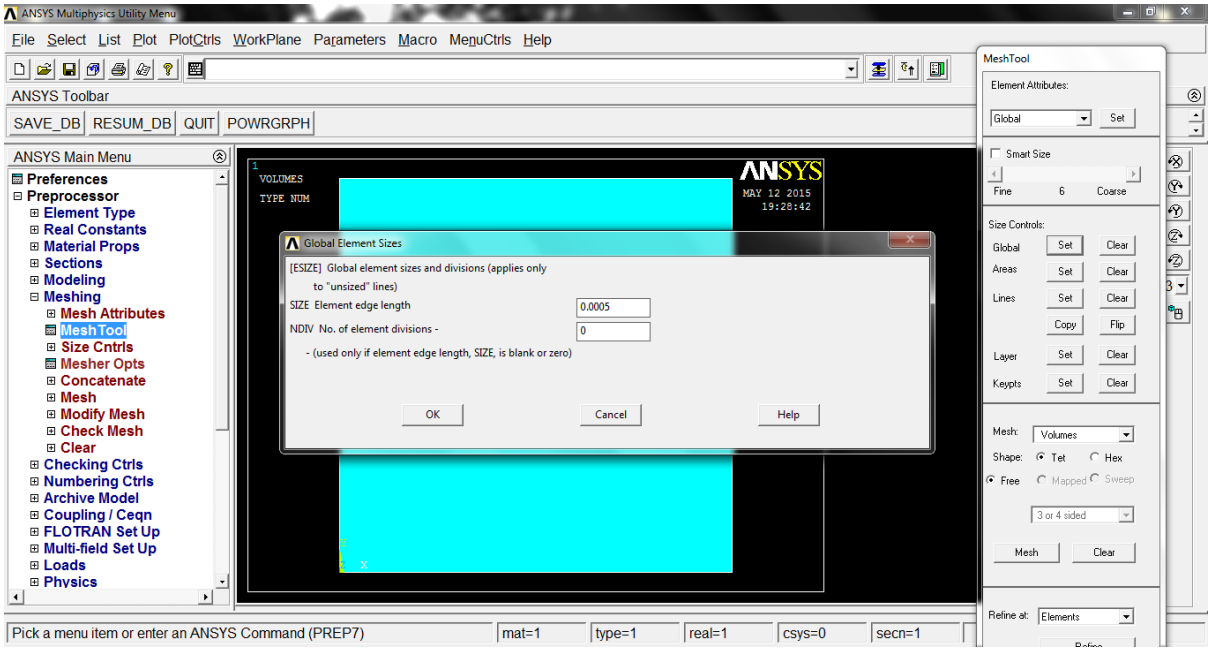

9. Meshing →Mesh Tool →Choose Global Set from Size Controls →Enter the value →Ok

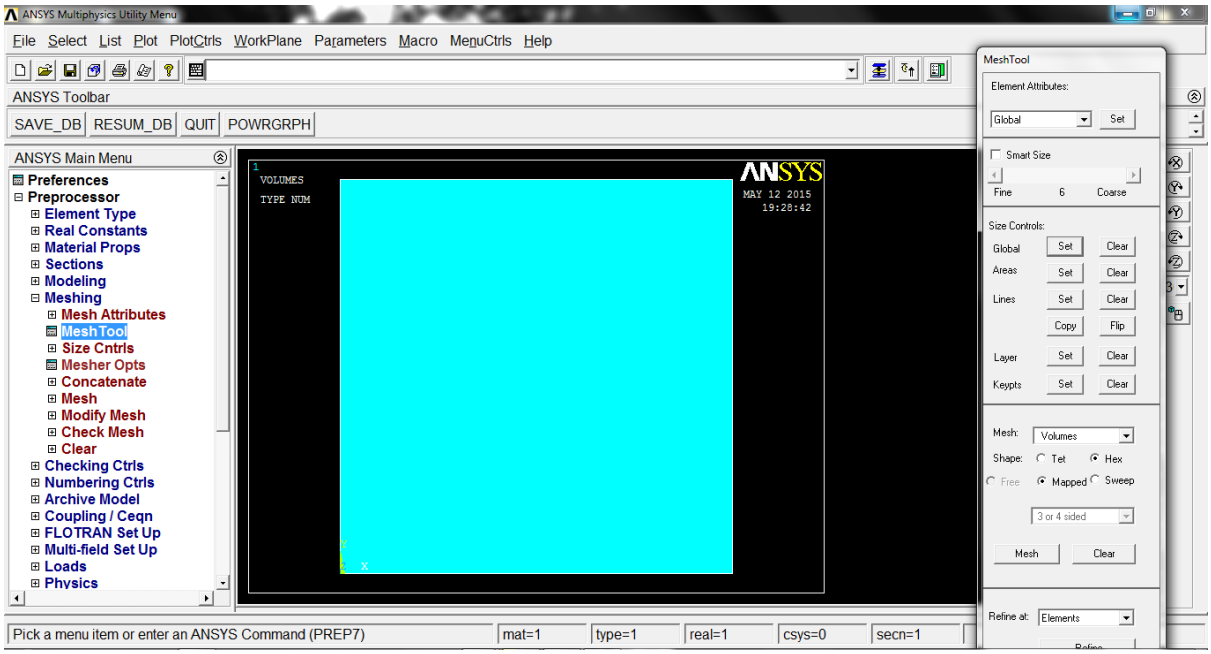

10. Choose Hex option as Shape

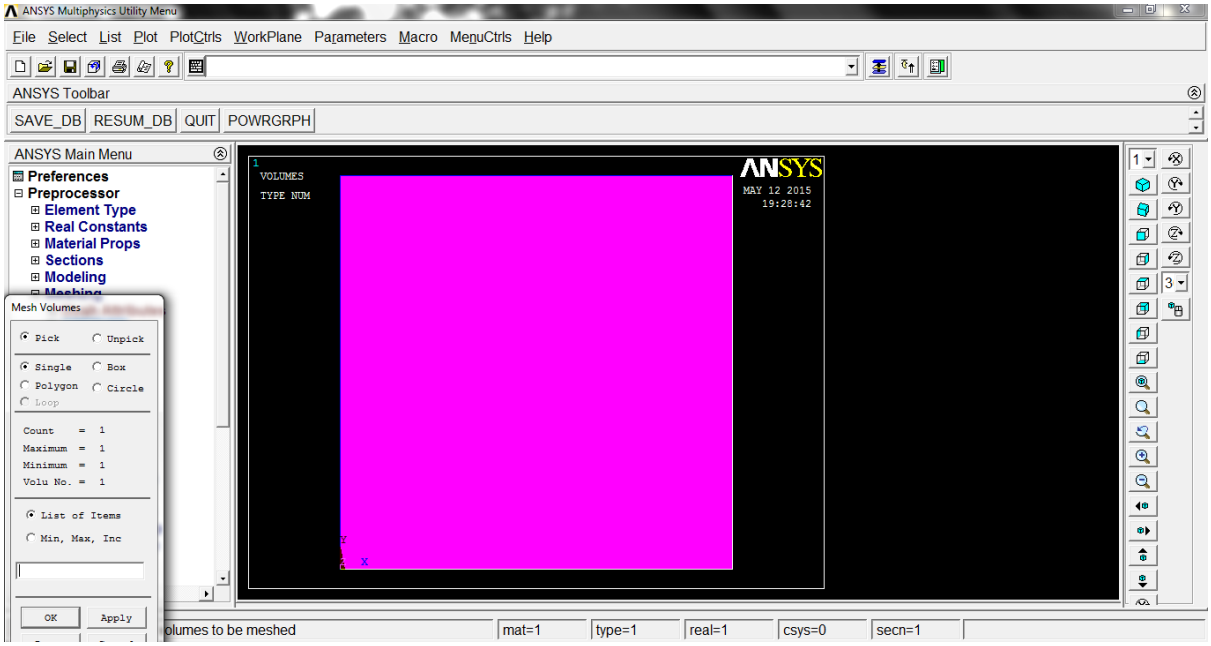

11. Click on Mesh →Pick the volume →Ok

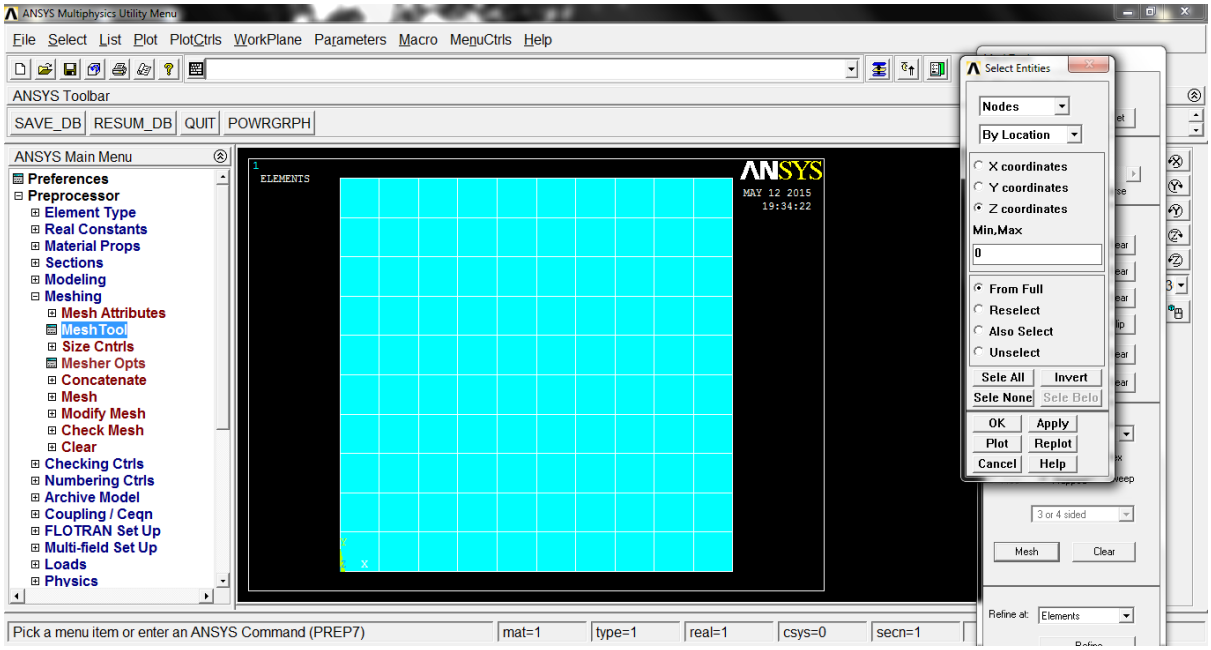

12. Choose Entities from the Select menu →Choose Select Nodes By Location (Z coordinates) →Enter the value →Ok

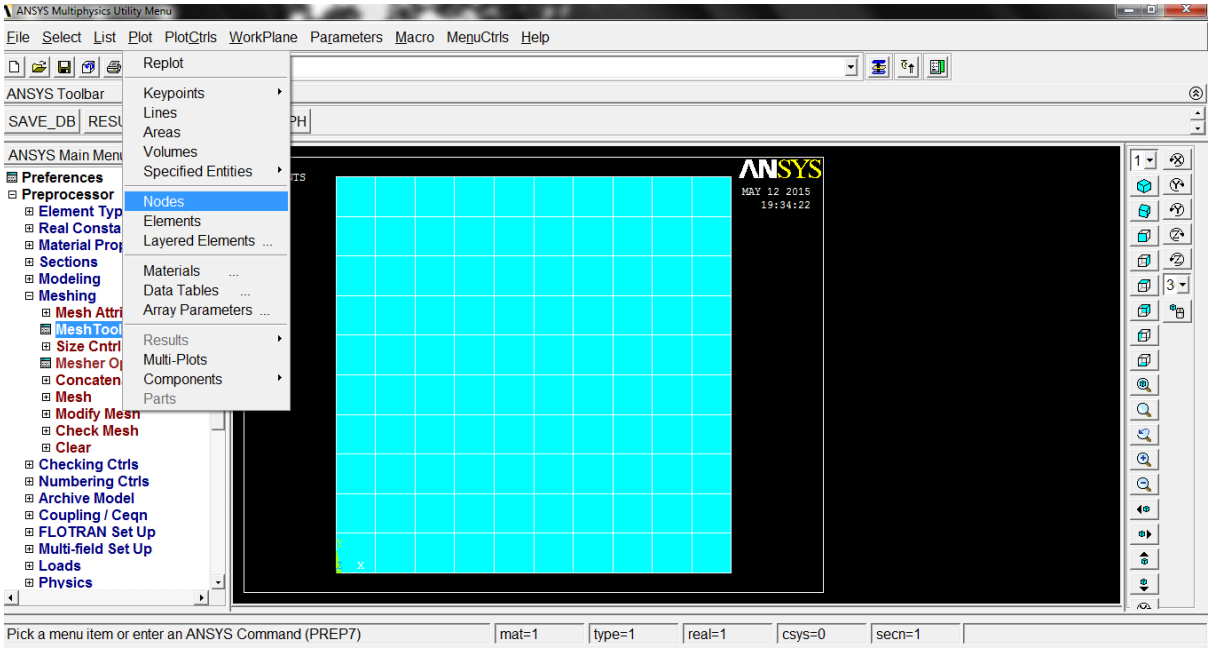

13. Choose Nodes from the Plot menu

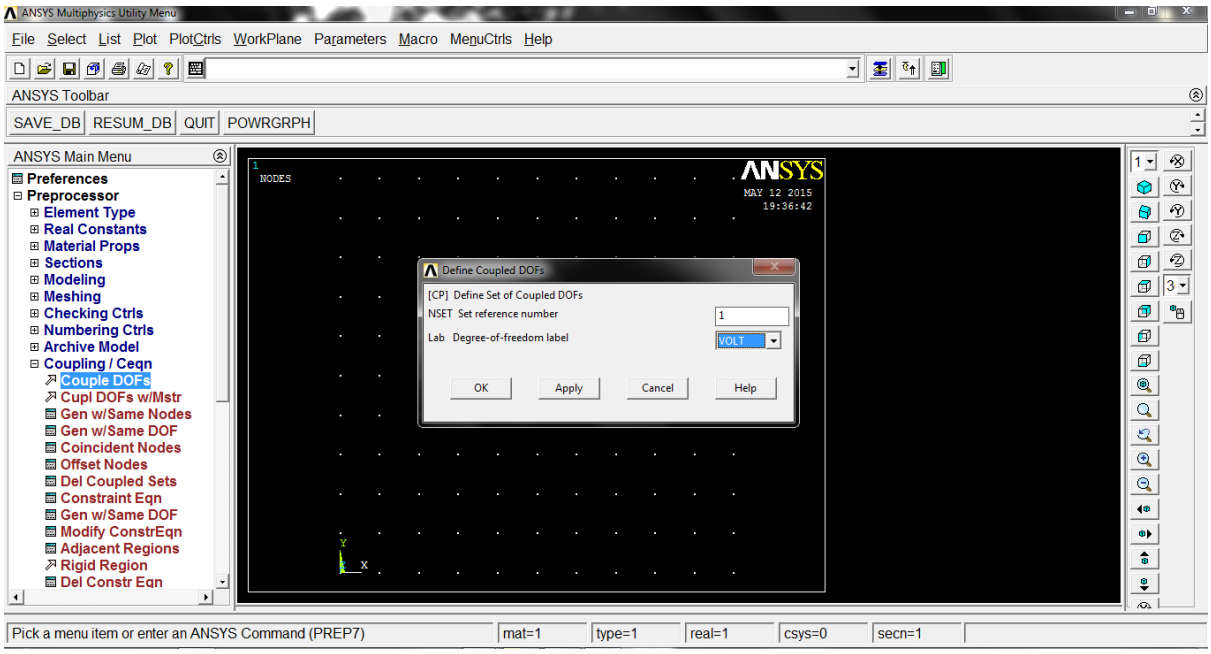

14. Coupling / Ceqn →Couple DOFs →Select Volt in the Degree of Freedom Label →Ok

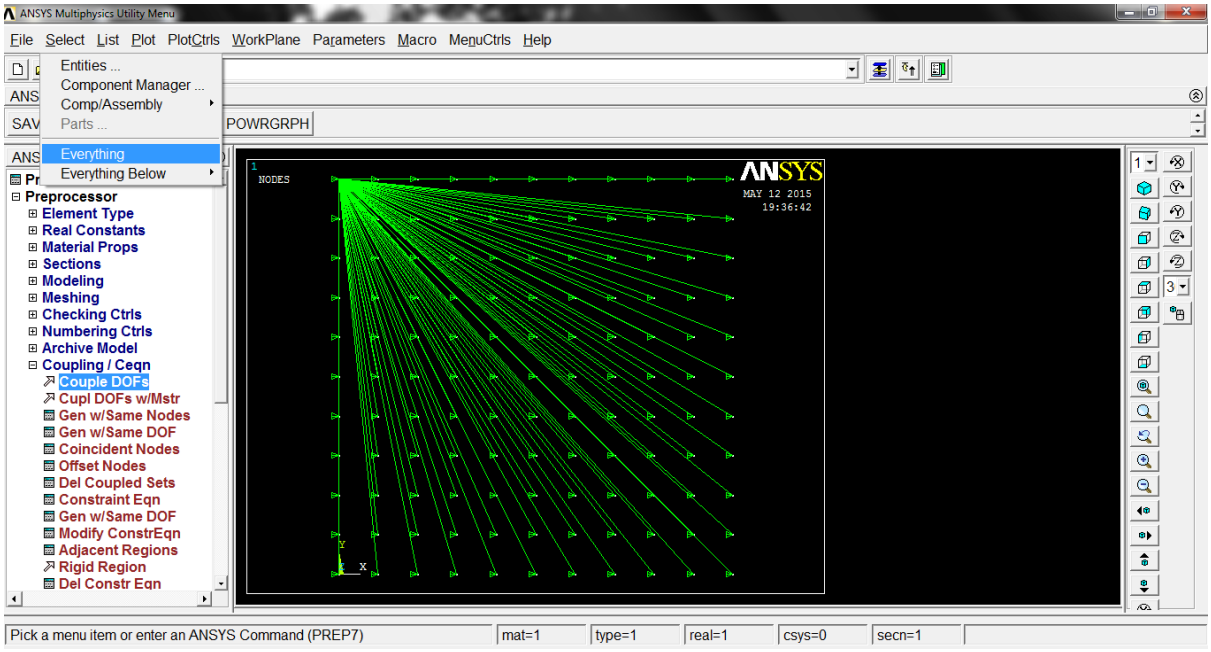

15. Choose Everything from the Select menu

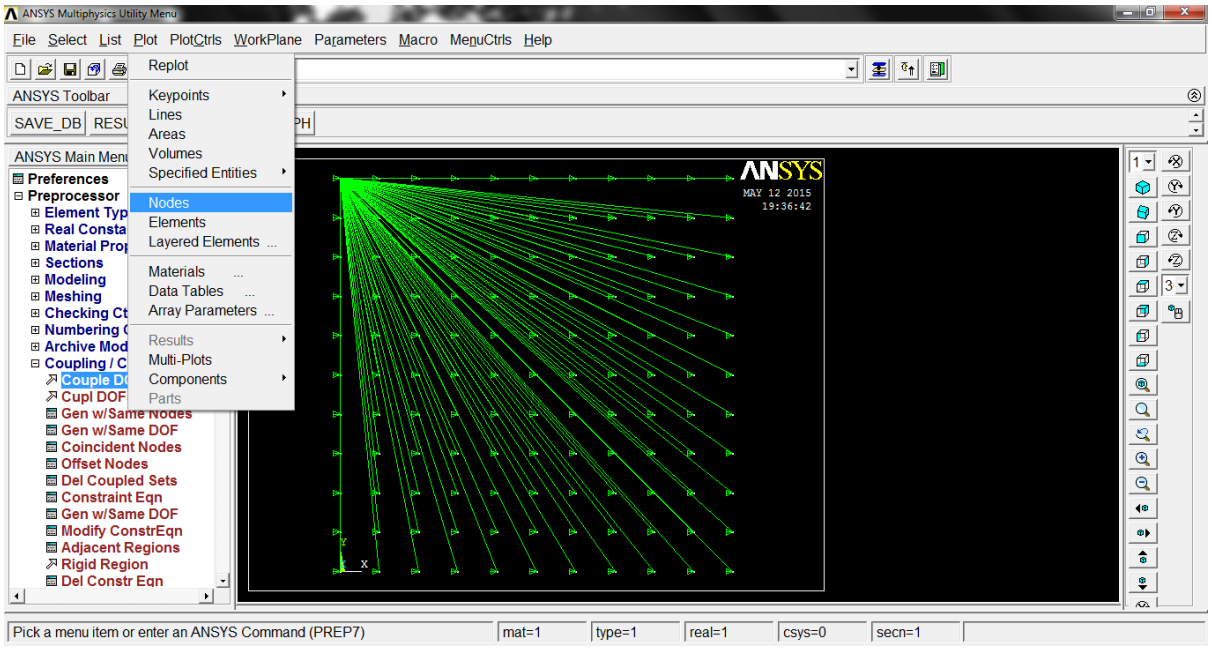

16. Select Nodes from the Plot menu

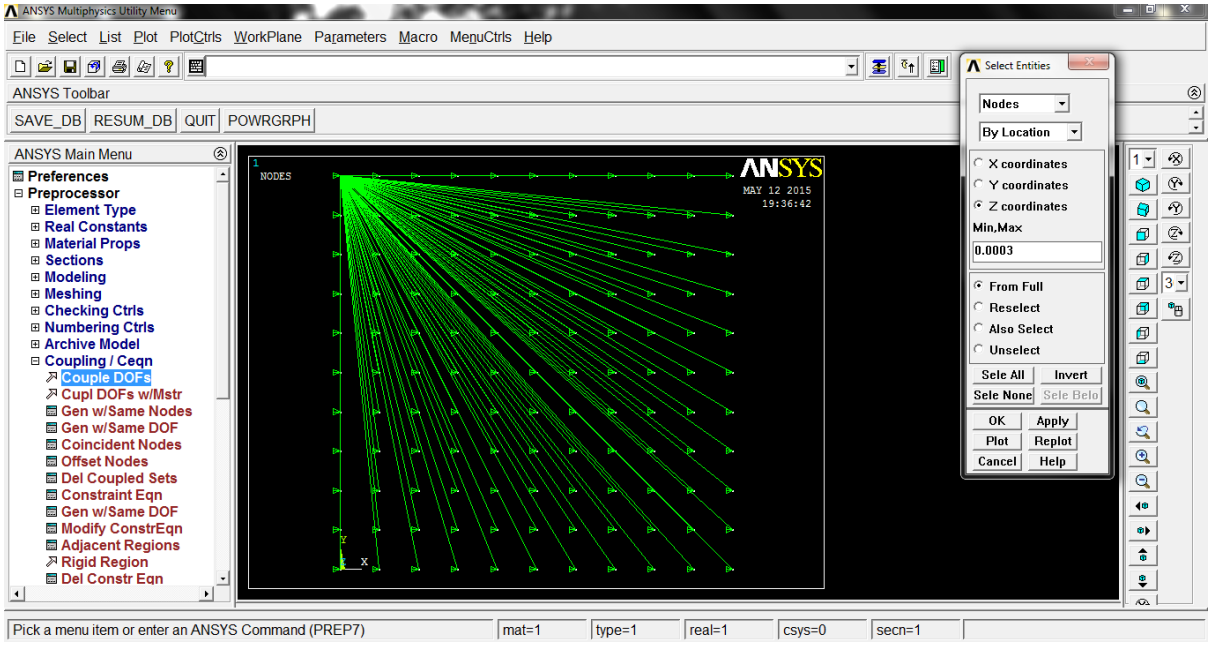

17. Choose Entities from the Select menu →Choose Select Nodes By Location (Z coordinates) →Enter the value →Ok

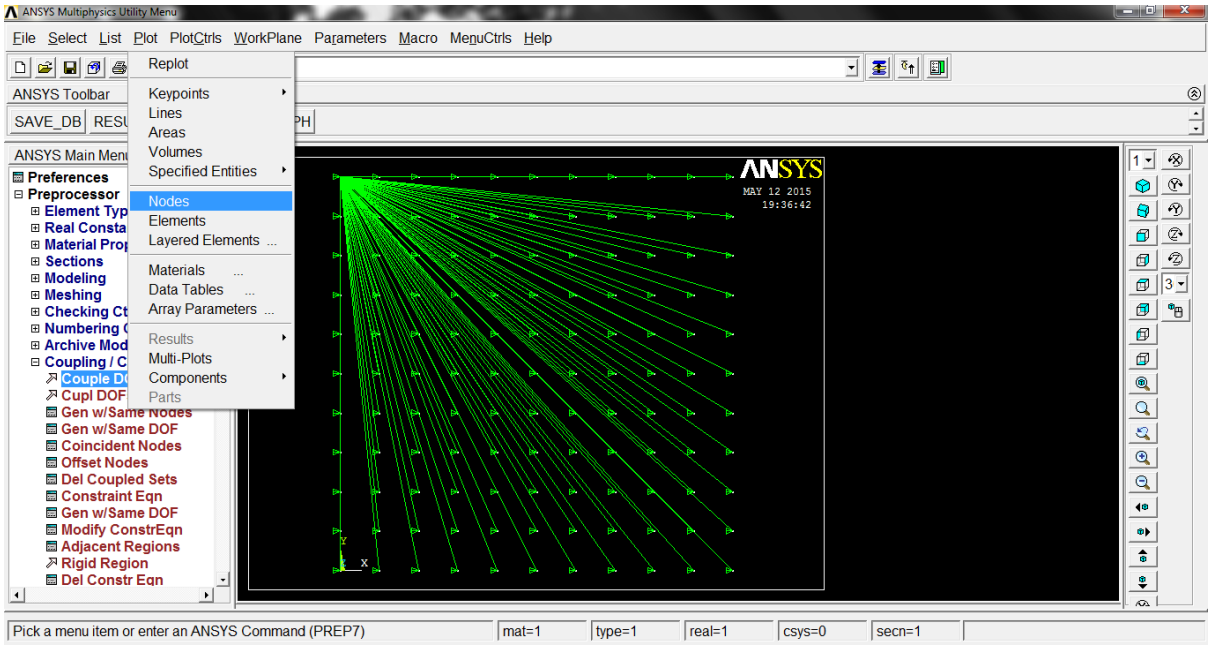

18. Select Nodes from the Plot menu

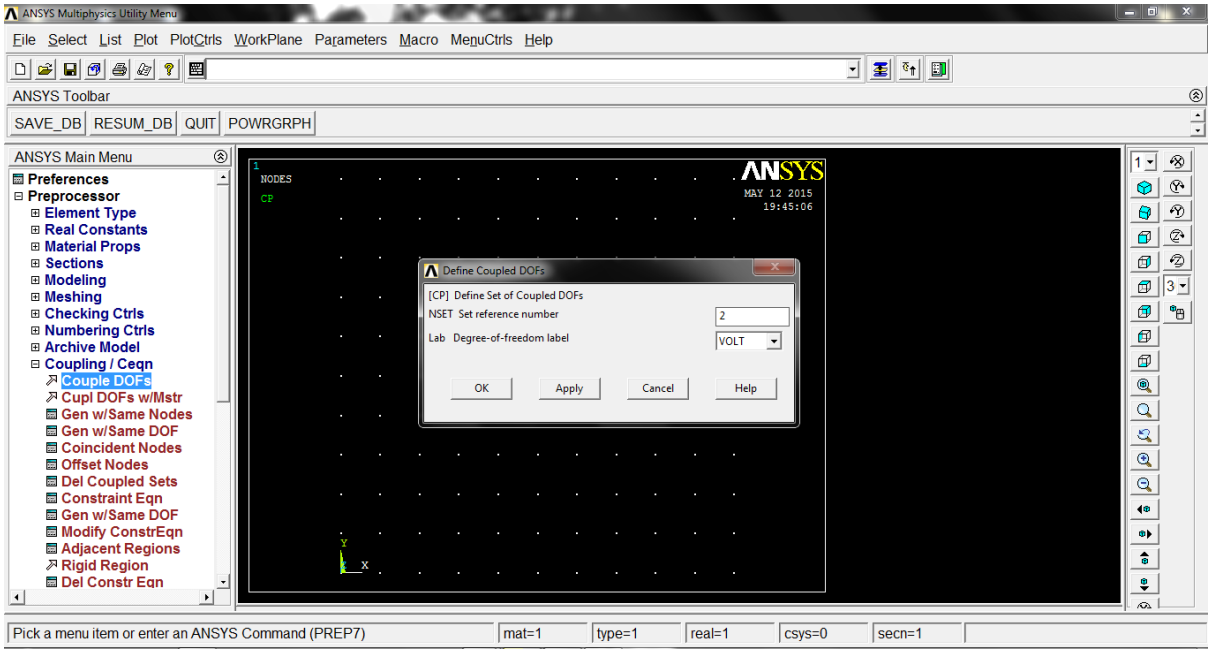

19. Coupling / Ceqn →Couple DOFs →Select Volt in the Degree of Freedom Label →Ok

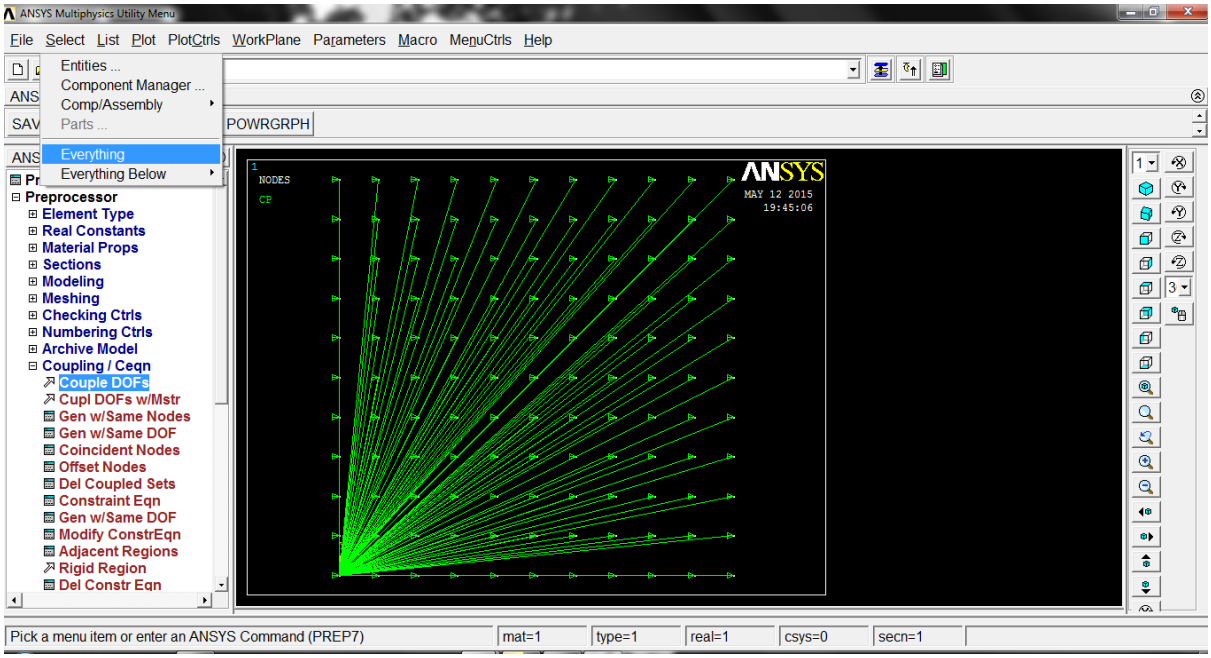

20. Choose Everything from the Select menu

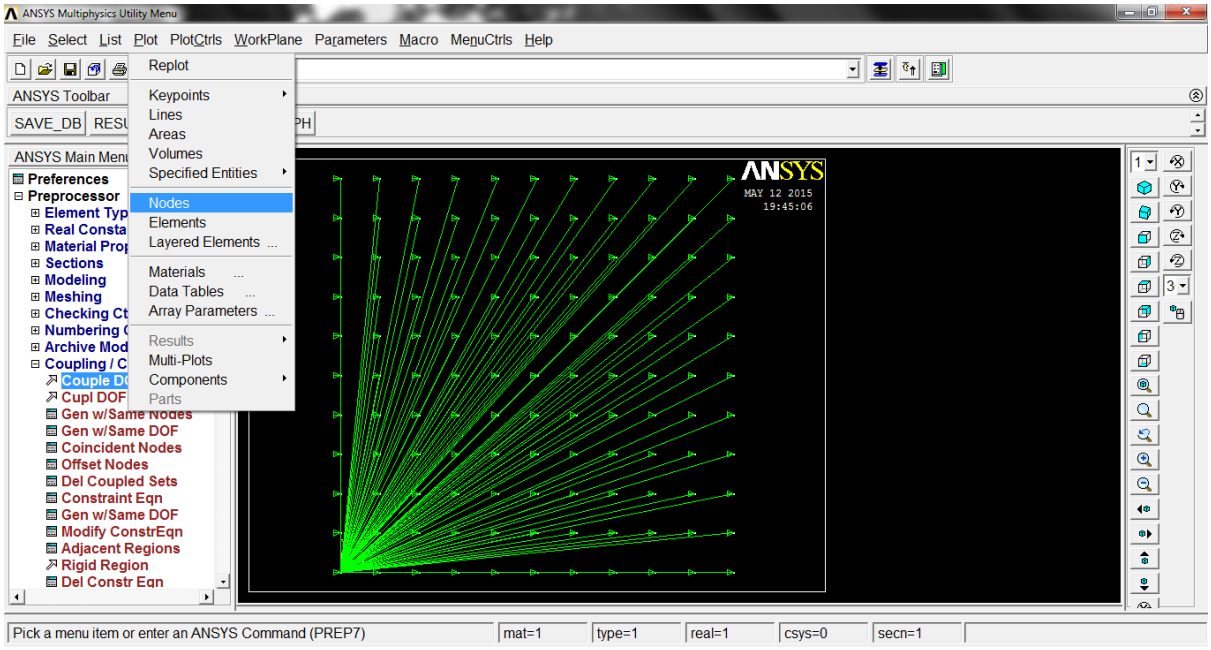

21. Select Nodes from the Plot menu

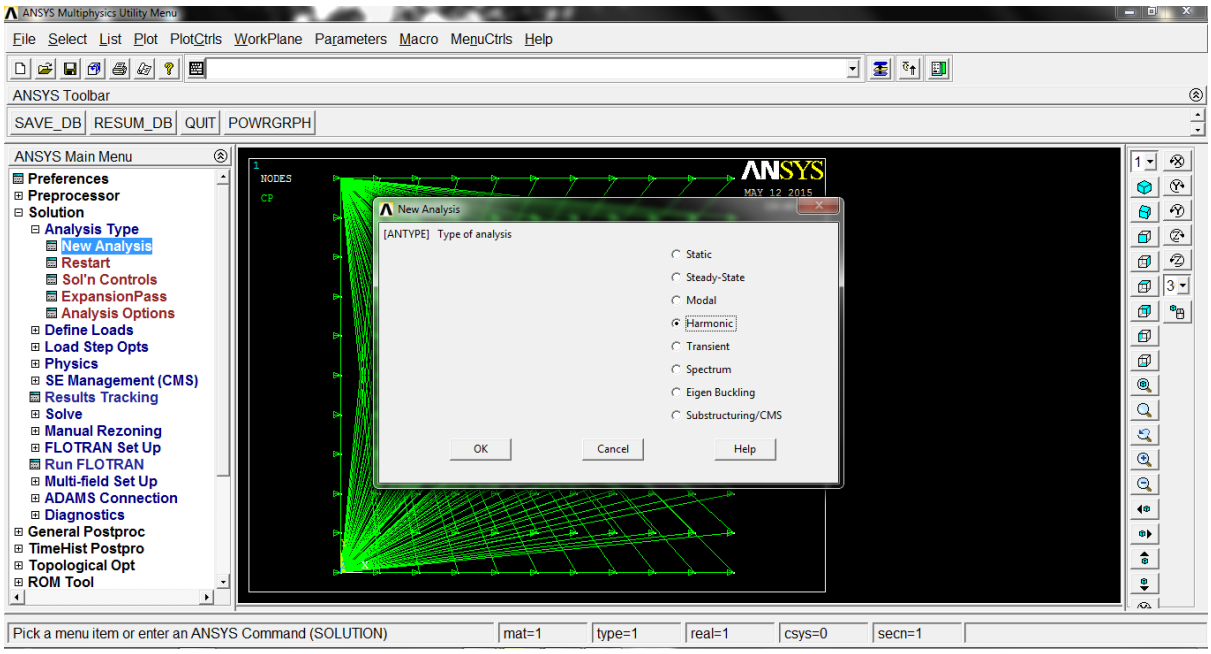

22. Solution →New Analysis →Choose Harmonic from the Type of analysis list →Ok

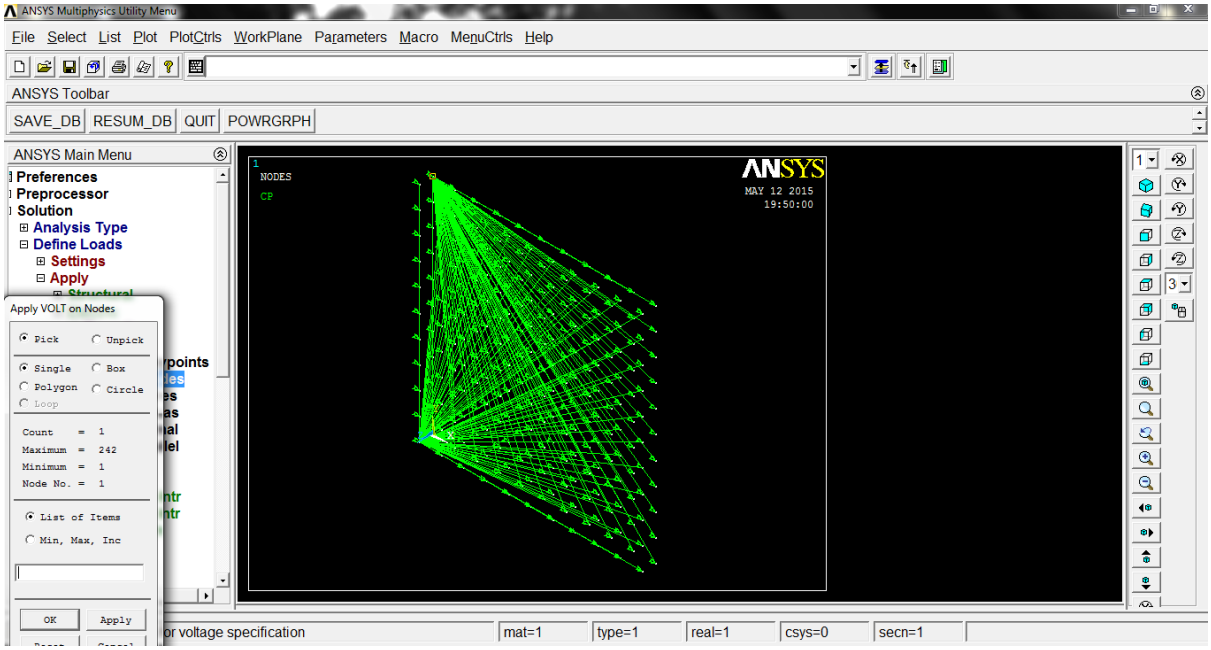

23. Solution →Define Loads →Apply →Electric →Boundary →Voltage →On Nodes →Select the node as shown in figure →Ok

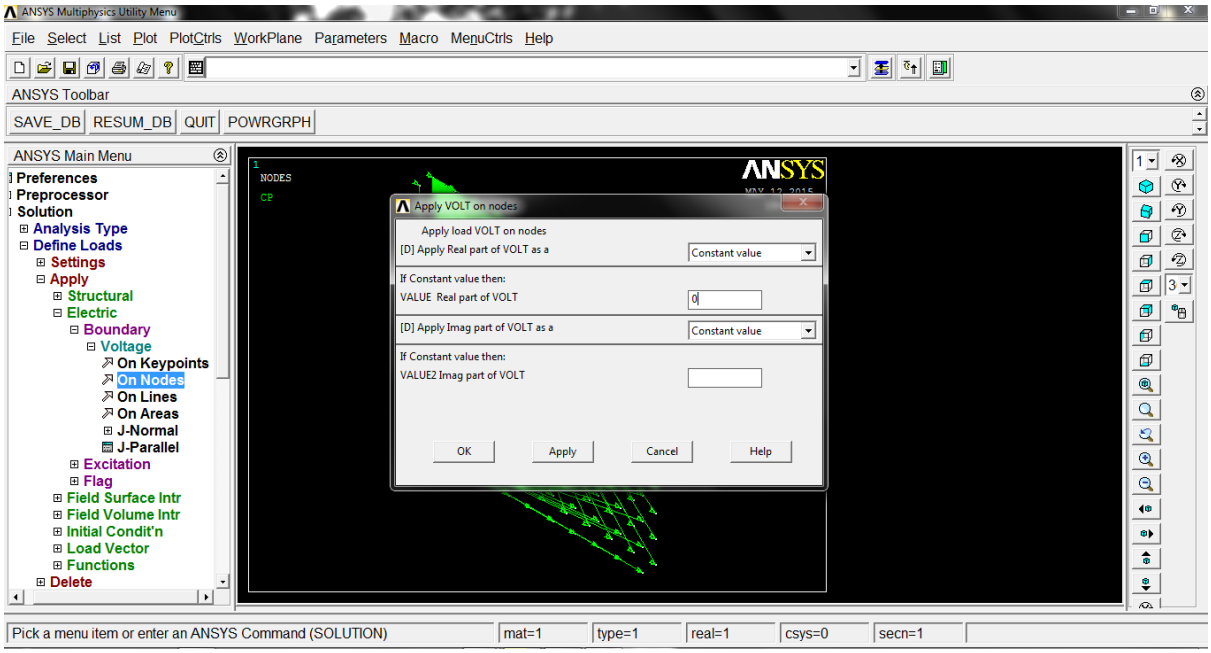

24. Enter the value →Ok

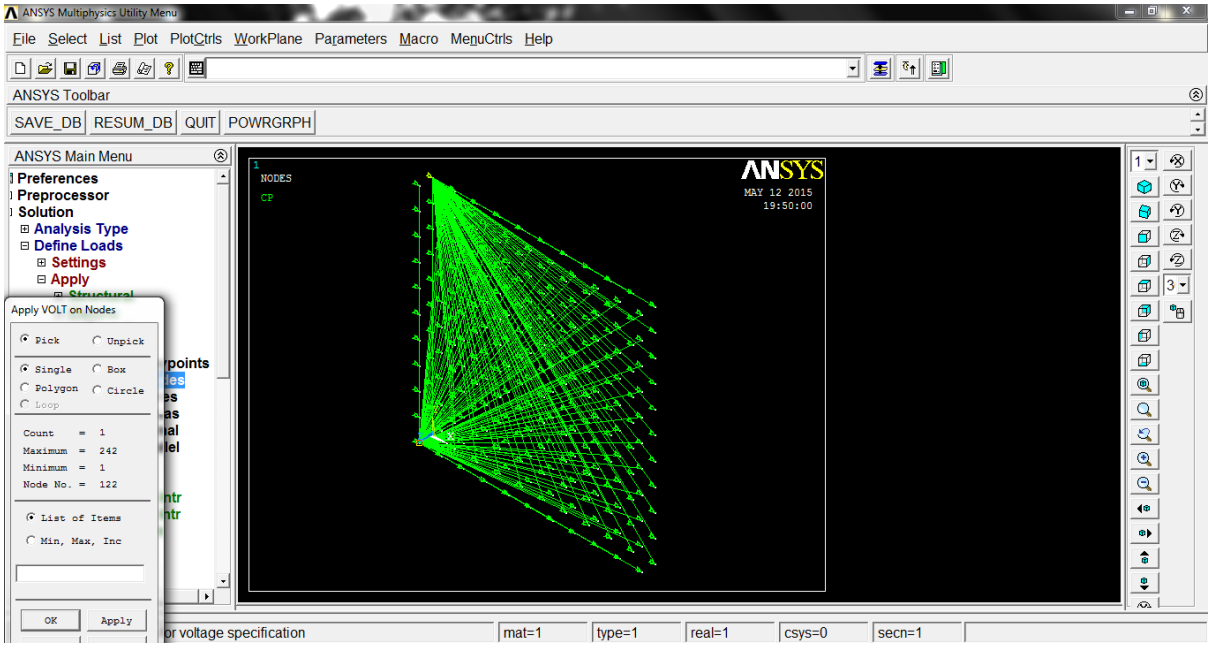

25. Solution →Define Loads →Apply →Electric →Boundary →Voltage →On Nodes →Select the node as shown in figure →Ok

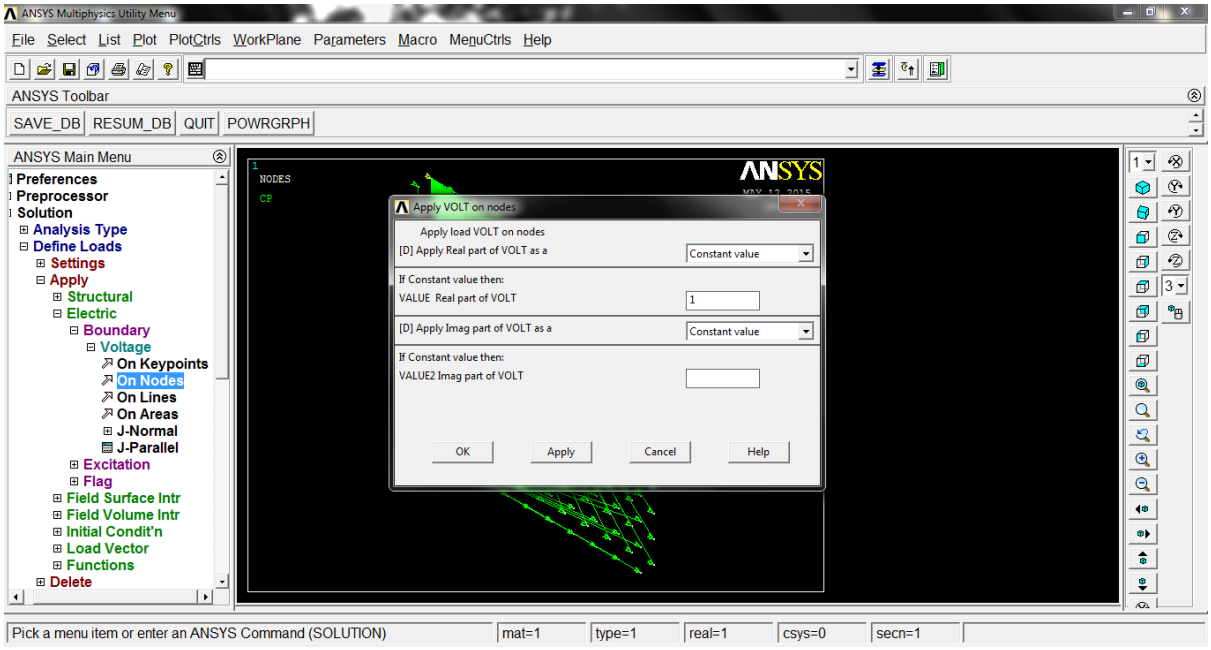

26. Enter the value →Ok

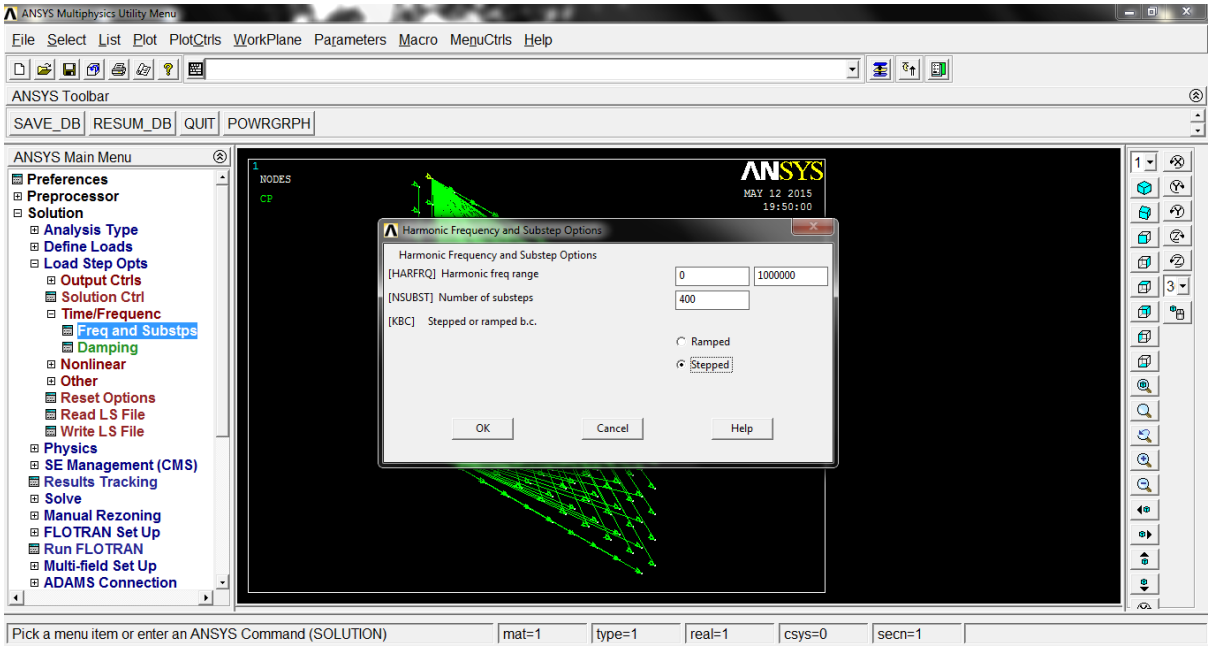

27. Solution →Load Step Opts →Time/Frequency →Freq and Substps →Enter the value →Choose Stepped →Ok

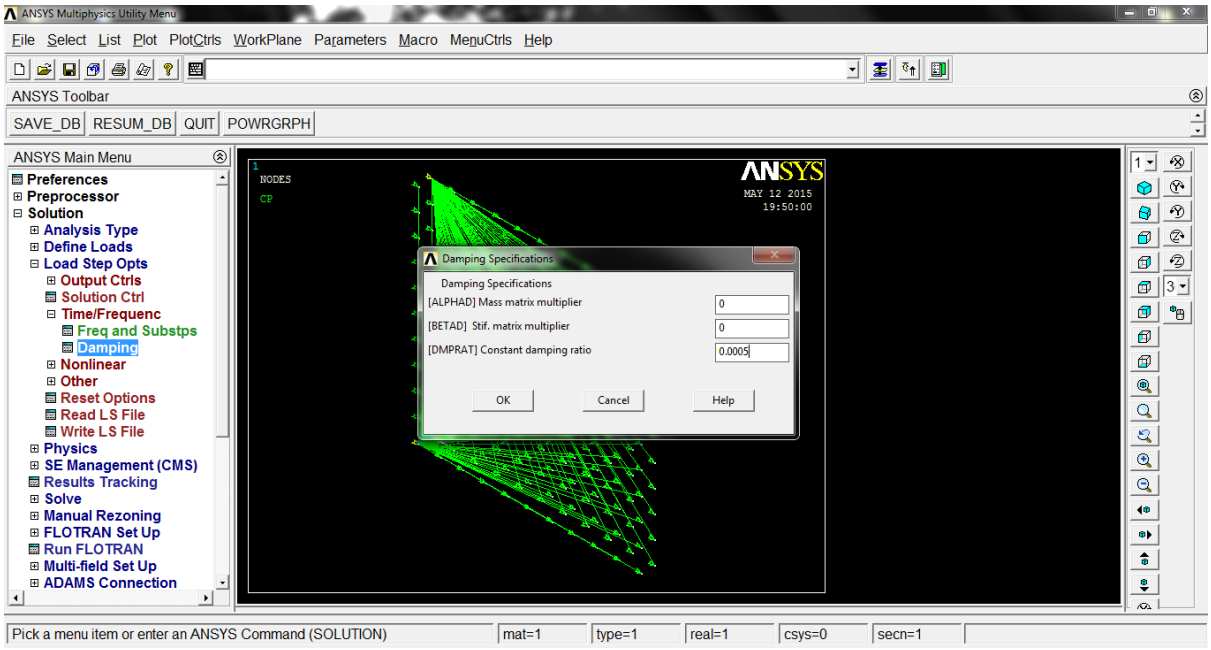

28. Solution →Load Step Opts →Time/Frequency →Damping →Enter the value →Ok

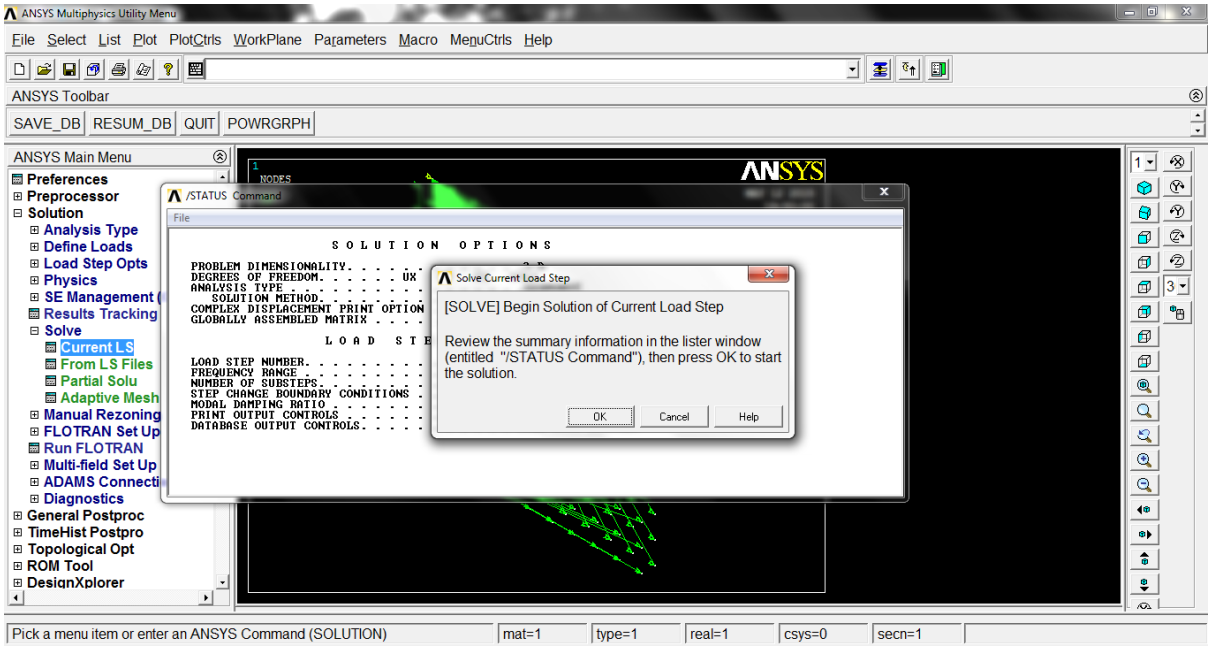

29. Solution →Solve →Current LS →Ok

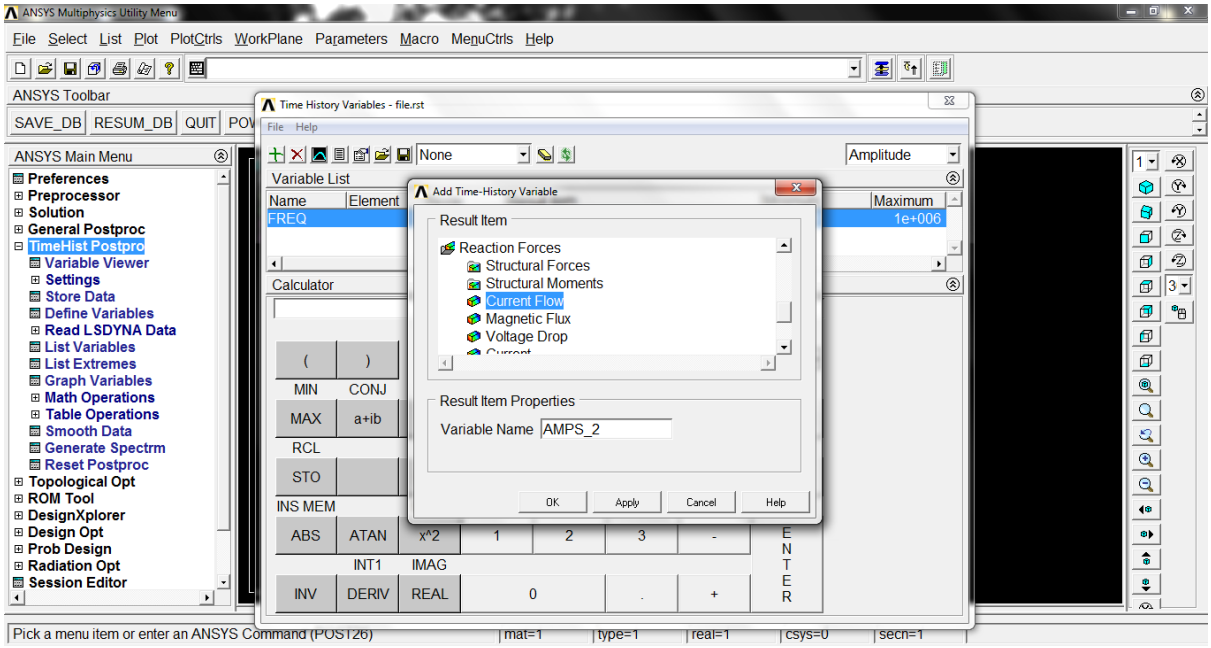

30. TimeHist Postpro →Add data →Select Current flow under Reaction Forces →Ok →Graph data

MODELLING OF PZT- STRUCTURE INTERACTION:

After the finite element modelling of a freely suspended PZT patch under harmonic excitation of up to 1000 kHz, the model was extended to simulate the interaction of a PZT with the host structure. The modelling procedure is similar with that of the freely suspended PZT patch.

CHAPTER 5

RESULTS AND DISCUSSION

A freely suspended PZT patch without the presence of the host structure with dimensions 10 mm ×10 mm × 0.3 mm was first modelled in the ANSYS 13 workspace, as depicted schematically in figure 1. The material properties were assigned to the PZT patch as given in Table 5.1.

Table 5.1: Material properties of the PZT patch

Parameters	Symbols	Values	Unit
Density	ρ	7600	Kg/m^3
Compliance	S_{11}	$9.7x10^{10}$	N/m^2
	S_{22}	$9.7x10^{10}$	
	S_{33}	$8.4x10^{10}$	
	S_{12}	$4.9x10^{10}$	
	S_{13}	$4.4x10^{10}$	
	S_{23}	$4.4x10^{10}$	
	S_{44}	$2.4x10^{10}$	
	S_{55}	$2.2x10^{10}$	
	S_{66}	$2.2x10^{10}$	
Electric permittivity	ε_{11}^T	947	Fm^{-1}
	ε_{22}^T	947	
	ε_{33}^T	605	
Piezoelectric strain coefficients	d_{31}	-8.02	m/V
	d_{32}	-8.02	
	d_{33}	18.31	
	d_{24}	12.84	
	d_{51}	12.84	

The PZT patch was excited along the z-direction by applying an alternating sinusoidal voltage of magnitude 1 V. It should be noted that, since the geometrical shapes and loadings are symmetrical in nature, only one quarter of the patch is modelled. That means the interfacial

nodes along the *x*-plane were restrained in the *x*-direction and those along the *y*-plane were restrained in the *y*-direction.

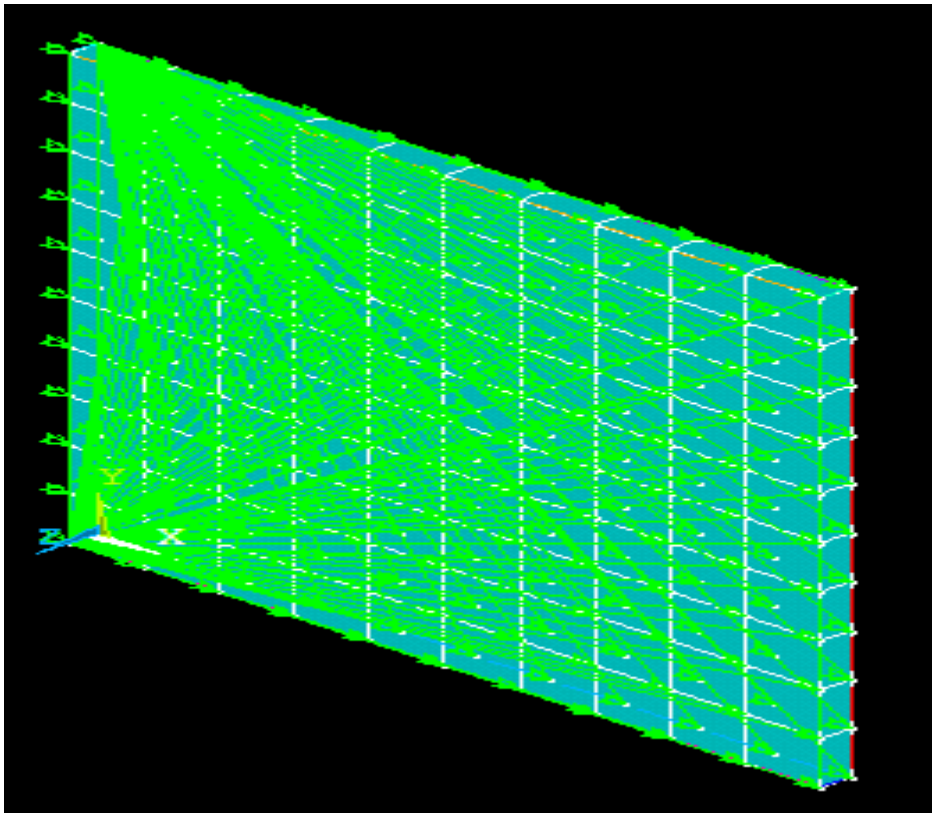

Figure 5.1: Model of the meshed PZT patch

The solution was obtained for a frequency range of 0-1000khz.The frequency range was divided into 400 sub steps and reaction charge was obtained for every sub step. The solution i.e. the reaction charge for the corresponding operating frequency is shown in Table 5.2. Then a graph between reaction charge and operating frequency was plotted. The graph is shown in Figure 5.2.

Table 5.2: Reaction charge corresponding to the operating frequency

FREQUENCY	REACTION CHARGE	
	REAL	IMAGINARY
2500	-2.36E-12	1.08E-36
5000	-2.36E-12	1.08E-36
7500	-2.36E-12	1.08E-36
10000	-2.36E-12	1.08E-36
12500	-2.36E-12	1.08E-36
15000	-2.36E-12	1.08E-36
17500	-2.36E-12	1.08E-36
20000	-2.36E-12	1.08E-36
22500	-2.36E-12	1.08E-36
25000	-2.36E-12	1.08E-36
27500	-2.36E-12	1.08E-36
30000	-2.36E-12	1.08E-36
32500	-2.36E-12	1.08E-36
35000	-2.36E-12	1.08E-36
37500	-2.36E-12	1.08E-36
40000	-2.36E-12	1.08E-36
42500	-2.36E-12	1.08E-36
45000	-2.36E-12	1.08E-36
47500	-2.36E-12	1.08E-36
50000	-2.36E-12	1.08E-36
52500	-2.36E-12	1.08E-36
55000	-2.36E-12	1.08E-36
57500	-2.36E-12	1.08E-36
60000	-2.36E-12	1.08E-36
62500	-2.36E-12	1.08E-36
65000	-2.36E-12	1.08E-36
67500	-2.36E-12	1.08E-36
70000	-2.36E-12	1.08E-36
72500	-2.36E-12	1.08E-36
75000	-2.36E-12	1.08E-36
77500	-2.36E-12	1.08E-36
80000	-2.36E-12	1.08E-36
82500	-2.36E-12	1.08E-36
85000	-2.36E-12	1.08E-36
87500	-2.36E-12	1.08E-36
90000	-2.36E-12	1.08E-36
92500	-2.36E-12	1.08E-36
95000	-2.36E-12	1.08E-36

97500	-2.36E-12	1.08E-36
100000	-2.36E-12	6.04E-36
102500	-2.36E-12	1.08E-36
105000	-2.36E-12	1.08E-36
107500	-2.36E-12	1.08E-36
110000	-2.36E-12	1.08E-36
112500	-2.36E-12	1.08E-36
115000	-2.36E-12	1.08E-36
117500	-2.36E-12	1.09E-36
120000	-2.36E-12	9.40E-36
122500	-2.36E-12	1.09E-36
125000	-2.36E-12	1.08E-36
127500	-2.36E-12	1.08E-36
130000	-2.36E-12	1.08E-36
132500	-2.36E-12	1.08E-36
135000	-2.36E-12	1.08E-36
137500	-2.36E-12	1.08E-36
140000	-2.36E-12	1.08E-36
142500	-2.36E-12	1.08E-36
145000	-2.36E-12	1.08E-36
147500	-2.36E-12	1.08E-36
150000	-2.36E-12	1.08E-36
152500	-2.36E-12	1.08E-36
155000	-2.36E-12	1.09E-36
157500	-2.36E-12	1.11E-36
160000	-2.36E-12	1.16E-36
162500	-2.36E-12	1.14E-36
165000	-2.36E-12	1.11E-36
167500	-2.36E-12	1.09E-36
170000	-2.36E-12	1.09E-36
172500	-2.36E-12	1.09E-36
175000	-2.36E-12	1.08E-36
177500	-2.36E-12	1.08E-36
180000	-2.36E-12	1.09E-36
182500	-2.36E-12	1.09E-36
185000	-2.36E-12	1.09E-36
187500	-2.36E-12	1.10E-36
190000	-2.36E-12	5.94E-36
192500	-2.36E-12	1.12E-36
195000	-2.36E-12	1.09E-36
197500	-2.36E-12	1.09E-36
200000	-2.36E-12	1.09E-36
202500	-2.36E-12	1.10E-36
205000	-2.36E-12	1.24E-36

207500	-2.36E-12	1.16E-36
210000	-2.36E-12	1.10E-36
212500	-2.36E-12	1.09E-36
215000	-2.36E-12	1.09E-36
217500	-2.36E-12	1.09E-36
220000	-2.36E-12	1.09E-36
222500	-2.36E-12	1.09E-36
225000	-2.36E-12	1.10E-36
227500	-2.36E-12	1.21E-36
230000	-2.36E-12	1.33E-36
232500	-2.36E-12	1.11E-36
235000	-2.36E-12	1.11E-36
237500	-2.36E-12	6.32E-36
240000	-2.36E-12	1.11E-36
242500	-2.36E-12	1.33E-36
245000	-2.36E-12	1.10E-36
247500	-2.36E-12	1.11E-36
250000	-2.36E-12	1.15E-36
252500	-2.36E-12	2.40E-36
255000	-2.36E-12	1.26E-36
257500	-2.36E-12	1.12E-36
260000	-2.36E-12	1.10E-36
262500	-2.36E-12	1.10E-36
265000	-2.36E-12	1.09E-36
267500	-2.36E-12	1.09E-36
270000	-2.36E-12	1.09E-36
272500	-2.36E-12	1.10E-36
275000	-2.36E-12	1.13E-36
277500	-2.36E-12	1.12E-36
280000	-2.36E-12	1.24E-36
282500	-2.36E-12	1.10E-36
285000	-2.36E-12	1.10E-36
287500	-2.36E-12	1.10E-36
290000	-2.36E-12	1.11E-36
292500	-2.36E-12	1.92E-36
295000	-2.36E-12	1.13E-36
297500	-2.36E-12	1.11E-36
300000	-2.36E-12	1.11E-36
302500	-2.36E-12	1.12E-36
305000	-2.36E-12	1.18E-36
307500	-2.36E-12	1.17E-36
310000	-2.36E-12	1.39E-36
312500	-2.36E-12	4.03E-36
315000	-2.36E-12	1.63E-36

317500	-2.36E-12	6.64E-36
320000	-2.36E-12	2.61E-36
322500	-2.36E-12	1.47E-36
325000	-2.36E-12	1.18E-36
327500	-2.36E-12	1.14E-36
330000	-2.36E-12	1.12E-36
332500	-2.36E-12	1.12E-36
335000	-2.36E-12	1.13E-36
337500	-2.36E-12	1.17E-36
340000	-2.36E-12	1.53E-36
342500	-2.36E-12	2.13E-36
345000	-2.36E-12	1.19E-36
347500	-2.36E-12	1.13E-36
350000	-2.36E-12	1.12E-36
352500	-2.36E-12	1.12E-36
355000	-2.36E-12	1.14E-36
357500	-2.36E-12	1.19E-36
360000	-2.36E-12	1.85E-36
362500	-2.36E-12	1.90E-36
365000	-2.36E-12	1.19E-36
367500	-2.36E-12	1.13E-36
370000	-2.36E-12	1.12E-36
372500	-2.36E-12	1.11E-36
375000	-2.36E-12	1.11E-36
377500	-2.36E-12	1.11E-36
380000	-2.36E-12	1.11E-36
382500	-2.36E-12	1.11E-36
385000	-2.36E-12	1.11E-36
387500	-2.36E-12	1.12E-36
390000	-2.36E-12	1.12E-36
392500	-2.36E-12	1.14E-36
395000	-2.36E-12	1.18E-36
397500	-2.36E-12	1.48E-36
400000	-2.36E-12	4.77E-36
402500	-2.36E-12	1.28E-36
405000	-2.36E-12	1.24E-36
407500	-2.36E-12	1.62E-36
410000	-2.36E-12	4.07E-36
412500	-2.36E-12	1.28E-36
415000	-2.36E-12	1.20E-36
417500	-2.36E-12	1.22E-36
420000	-2.36E-12	1.41E-36
422500	-2.36E-12	2.08E-35
425000	-2.36E-12	2.31E-36

427500	-2.36E-12	1.07E-35
430000	-2.36E-12	1.53E-36
432500	-2.36E-12	1.25E-36
435000	-2.36E-12	1.19E-36
437500	-2.36E-12	1.19E-36
440000	-2.36E-12	1.27E-36
442500	-2.36E-12	9.74E-36
445000	-2.36E-12	1.33E-36
447500	-2.36E-12	1.21E-36
450000	-2.36E-12	1.26E-36
452500	-2.36E-12	1.81E-36
455000	-2.36E-12	4.29E-36
457500	-2.36E-12	1.35E-36
460000	-2.36E-12	1.27E-36
462500	-2.36E-12	1.59E-36
465000	-2.36E-12	5.25E-36
467500	-2.36E-12	1.31E-36
470000	-2.36E-12	1.19E-36
472500	-2.36E-12	1.20E-36
475000	-2.36E-12	1.16E-36
477500	-2.36E-12	1.16E-36
480000	-2.36E-12	1.22E-36
482500	-2.36E-12	1.19E-36
485000	-2.36E-12	1.21E-36
487500	-2.36E-12	1.27E-36
490000	-2.36E-12	1.46E-36
492500	-2.36E-12	3.13E-36
495000	-2.36E-12	6.14E-36
497500	-2.36E-12	2.63E-36
500000	-2.36E-12	1.10E-35
502500	-2.36E-12	1.83E-36
505000	-2.36E-12	3.01E-36
507500	-2.36E-12	3.88E-36
510000	-2.36E-12	1.44E-36
512500	-2.36E-12	1.26E-36
515000	-2.36E-12	1.21E-36
517500	-2.36E-12	1.20E-36
520000	-2.36E-12	1.20E-36
522500	-2.36E-12	1.22E-36
525000	-2.36E-12	1.29E-36
527500	-2.36E-12	1.58E-36
530000	-2.36E-12	7.06E-36
532500	-2.36E-12	2.94E-36
535000	-2.36E-12	1.43E-36

537500	-2.36E-12	1.26E-36
540000	-2.36E-12	1.22E-36
542500	-2.36E-12	1.22E-36
545000	-2.36E-12	1.26E-36
547500	-2.36E-12	1.43E-36
550000	-2.36E-12	5.54E-36
552500	-2.36E-12	2.06E-36
555000	-2.36E-12	1.41E-36
557500	-2.36E-12	1.50E-36
560000	-2.36E-12	3.19E-36
562500	-2.36E-12	5.77E-36
565000	-2.36E-12	1.62E-36
567500	-2.36E-12	1.76E-36
570000	-2.36E-12	2.44E-36
572500	-2.36E-12	1.30E-36
575000	-2.36E-12	1.27E-36
577500	-2.36E-12	1.20E-36
580000	-2.36E-12	1.20E-36
582500	-2.36E-12	1.20E-36
585000	-2.36E-12	1.21E-36
587500	-2.36E-12	1.22E-36
590000	-2.36E-12	1.26E-36
592500	-2.36E-12	1.32E-36
595000	-2.36E-12	1.51E-36
597500	-2.36E-12	3.21E-36
600000	-2.36E-12	4.36E-36
602500	-2.36E-12	1.89E-35
605000	-2.36E-12	2.21E-36
607500	-2.36E-12	3.95E-36
610000	-2.36E-12	1.51E-35
612500	-2.36E-12	1.30E-35
615000	-2.36E-12	7.87E-36
617500	-2.36E-12	1.99E-36
620000	-2.36E-12	1.59E-36
622500	-2.36E-12	1.50E-36
625000	-2.36E-12	1.55E-36
627500	-2.36E-12	1.86E-36
630000	-2.36E-12	3.64E-36
632500	-2.36E-12	1.42E-34
635000	-2.36E-12	3.49E-36
637500	-2.36E-12	1.99E-36
640000	-2.36E-12	2.27E-36
642500	-2.36E-12	2.91E-35
645000	-2.36E-12	2.83E-36

647500	-2.36E-12	1.57E-36
650000	-2.36E-12	1.36E-36
652500	-2.36E-12	1.30E-36
655000	-2.36E-12	1.27E-36
657500	-2.36E-12	1.26E-36
660000	-2.36E-12	1.28E-36
662500	-2.36E-12	1.34E-36
665000	-2.36E-12	1.55E-36
667500	-2.36E-12	3.28E-36
670000	-2.36E-12	9.40E-36
672500	-2.36E-12	1.75E-36
675000	-2.36E-12	1.38E-36
677500	-2.36E-12	1.30E-36
680000	-2.36E-12	1.27E-36
682500	-2.36E-12	1.27E-36
685000	-2.36E-12	1.29E-36
687500	-2.36E-12	1.32E-36
690000	-2.36E-12	1.39E-36
692500	-2.36E-12	1.55E-36
695000	-2.36E-12	2.04E-36
697500	-2.36E-12	5.34E-36
700000	-2.36E-12	4.43E-35
702500	-2.36E-12	3.06E-36
705000	-2.36E-12	1.83E-36
707500	-2.36E-12	1.60E-36
710000	-2.36E-12	1.61E-36
712500	-2.36E-12	1.89E-36
715000	-2.36E-12	3.78E-36
717500	-2.36E-12	4.45E-35
720000	-2.36E-12	3.15E-36
722500	-2.36E-12	4.22E-36
725000	-2.36E-12	3.68E-35
727500	-2.36E-12	5.34E-36
730000	-2.36E-12	2.64E-36
732500	-2.36E-12	1.81E-36
735000	-2.36E-12	2.10E-36
737500	-2.36E-12	1.19E-35
740000	-2.36E-12	3.48E-36
742500	-2.36E-12	1.89E-36
745000	-2.36E-12	2.02E-36
747500	-2.36E-12	4.16E-36
750000	-2.36E-12	3.86E-35
752500	-2.36E-12	2.75E-36
755000	-2.36E-12	1.78E-36

757500	-2.36E-12	1.68E-36
760000	-2.36E-12	1.59E-36
762500	-2.36E-12	1.66E-36
765000	-2.36E-12	1.95E-36
767500	-2.36E-12	3.25E-36
770000	-2.36E-12	5.02E-36
772500	-2.36E-12	1.33E-34
775000	-2.36E-12	1.90E-35
777500	-2.36E-12	9.47E-36
780000	-2.36E-12	1.27E-34
782500	-2.36E-12	5.60E-36
785000	-2.36E-12	2.44E-36
787500	-2.36E-12	1.83E-36
790000	-2.36E-12	1.61E-36
792500	-2.36E-12	1.50E-36
795000	-2.36E-12	1.46E-36
797500	-2.36E-12	1.44E-36
800000	-2.36E-12	1.46E-36
802500	-2.36E-12	1.54E-36
805000	-2.36E-12	1.75E-36
807500	-2.36E-12	2.66E-36
810000	-2.36E-12	2.47E-35
812500	-2.36E-12	4.95E-36
815000	-2.36E-12	2.15E-36
817500	-2.36E-12	3.02E-36
820000	-2.36E-12	1.87E-36
822500	-2.36E-12	2.04E-36
825000	-2.36E-12	3.12E-36
827500	-2.36E-12	2.50E-35
830000	-2.36E-12	6.93E-36
832500	-2.36E-12	5.96E-36
835000	-2.36E-12	9.78E-35
837500	-2.36E-12	8.75E-36
840000	-2.36E-12	3.29E-36
842500	-2.36E-12	3.23E-36
845000	-2.36E-12	3.80E-35
847500	-2.36E-12	3.56E-36
850000	-2.36E-12	2.24E-36
852500	-2.36E-12	2.23E-36
855000	-2.36E-12	2.80E-36
857500	-2.36E-12	5.49E-36
860000	-2.36E-12	1.04E-34
862500	-2.36E-12	1.21E-34
865000	-2.36E-12	1.07E-35

867500	-2.36E-12	3.49E-36
870000	-2.36E-12	2.26E-36
872500	-2.36E-12	1.84E-36
875000	-2.36E-12	1.64E-36
877500	-2.36E-12	1.54E-36
880000	-2.36E-12	1.48E-36
882500	-2.36E-12	1.45E-36
885000	-2.36E-12	1.44E-36
887500	-2.36E-12	1.45E-36
890000	-2.36E-12	1.48E-36
892500	-2.36E-12	1.56E-36
895000	-2.36E-12	1.74E-36
897500	-2.36E-12	2.36E-36
900000	-2.36E-12	7.89E-36
902500	-2.36E-12	1.47E-35
905000	-2.36E-12	2.74E-36
907500	-2.36E-12	2.01E-36
910000	-2.36E-12	3.58E-36
912500	-2.36E-12	2.20E-36
915000	-2.36E-12	4.33E-36
917500	-2.36E-12	1.06E-35
920000	-2.36E-12	3.43E-36
922500	-2.36E-12	1.53E-35
925000	-2.36E-12	6.31E-36
927500	-2.36E-12	9.81E-36
930000	-2.36E-12	2.07E-34
932500	-2.36E-12	8.26E-36
935000	-2.36E-12	3.58E-36
937500	-2.36E-12	2.34E-36
940000	-2.36E-12	2.02E-36
942500	-2.36E-12	1.91E-36
945000	-2.36E-12	1.91E-36
947500	-2.36E-12	2.02E-36
950000	-2.36E-12	2.29E-36
952500	-2.36E-12	3.07E-36
955000	-2.36E-12	6.06E-36
957500	-2.36E-12	1.35E-35
960000	-2.36E-12	1.00E-34
962500	-2.36E-12	2.08E-35
965000	-2.36E-12	1.79E-34
967500	-2.36E-12	1.68E-35
970000	-2.36E-12	4.97E-36
972500	-2.36E-12	3.05E-36
975000	-2.36E-12	2.41E-36

977500	-2.36E-12	2.14E-36
980000	-2.36E-12	2.08E-36
982500	-2.36E-12	2.10E-36
985000	-2.36E-12	2.20E-36
987500	-2.36E-12	2.42E-36
990000	-2.36E-12	2.83E-36
992500	-2.36E-12	4.02E-36
995000	-2.36E-12	8.48E-36
997500	-2.36E-12	6.57E-35
1000000	-2.36E-12	3.92E-35

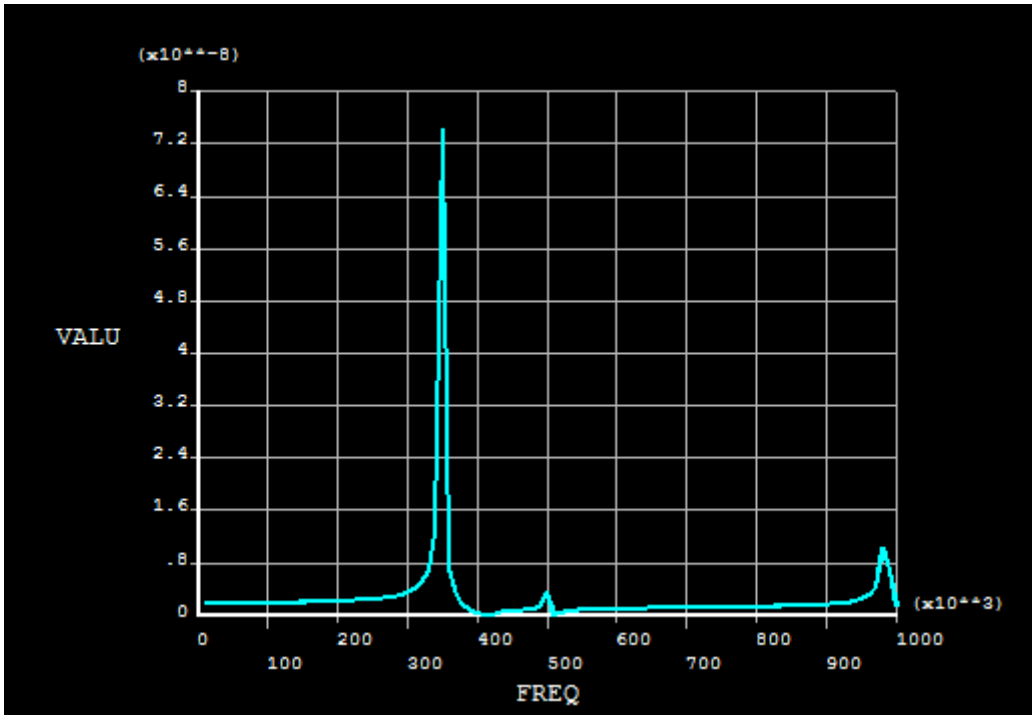

Figure 5.2: Plot between Reaction force and corresponding operating frequency

After modelling the PZT patch for a harmonic excitation with frequency up to 1000 kHz, the finite element model was extended to simulate the interaction of the PZT with the host structure.

A simple aluminium beam with rectangular cross section (dimensions-231 mm× 21 mm × 2 mm) was used as the test specimen in this study. A PZT patch of dimension 10 mm×10 mm×0.2 mm was also bonded at the middle of the beam. The test specimen was numerically modelled in the ANSYS 13 workspace as illustrated in Figure 5.3.

The material properties of the aluminium beam are listed in Table 5.3.

Table 5.3: Material properties of the Aluminium beam

Parameters	Symbols	Values	Unit
Density	ρ	2715	Kg/m^3
Poisson's ratio	v	0.3	--
Young's modulus (Isotropic)	Y	68.95	10^9 Nm^{-2}
Constant stiffness multiplier	β	$1x10^{-9}$	--

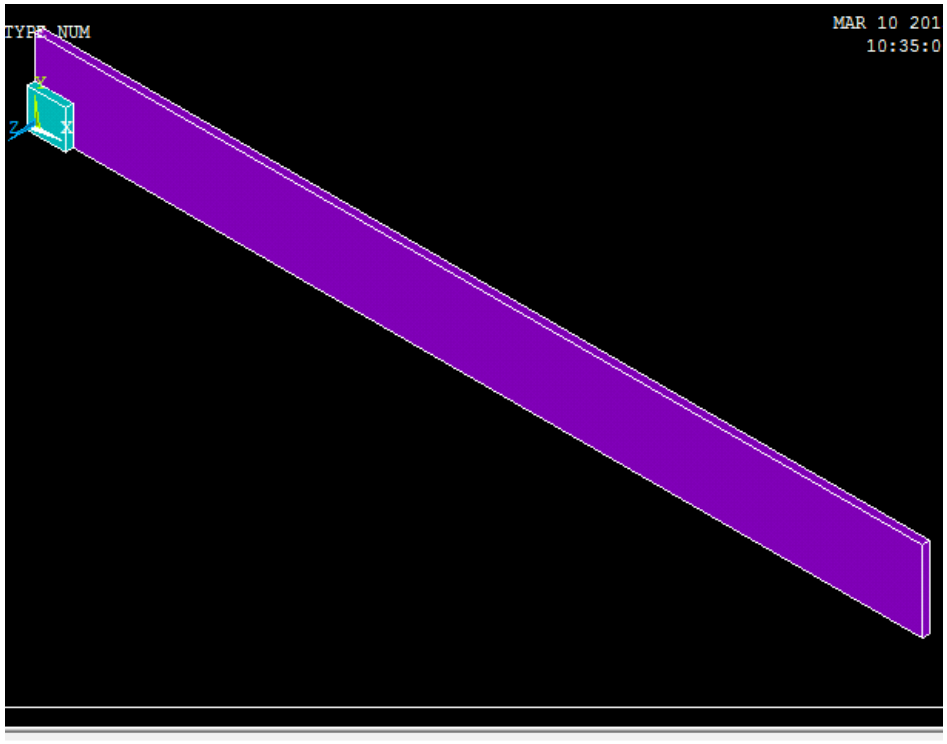

Figure 5.3: Modelling of one quarter of the aluminium beam

The reaction charge was obtained for the selected frequency range. From the reaction charge conductance of the structure was calculated with the help of the formula given in the formulation part. The conductance signature was obtained which is shown in Figure 5.4.

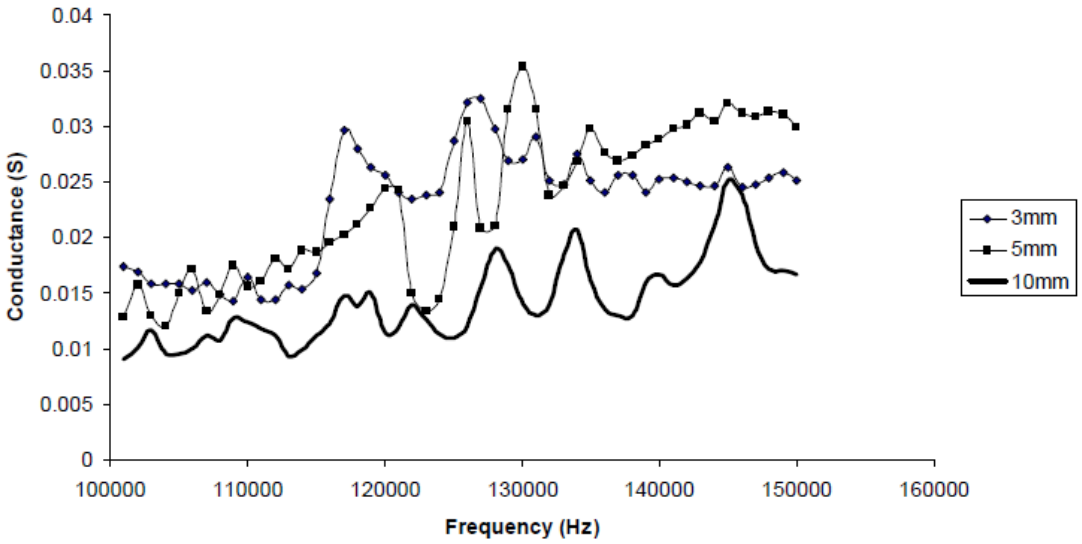

Figure 5.4: Conductance signature of the PZT-structure interaction using 3mm, 5mm, and 10mm element size

Comparing the conductance signatures of the undamaged structure with those of the damaged one, the presence of the damage in terms of its location and extent may be predicted.

CHAPTER 6

CONCLUSION

Structural Health Monitoring (SHM) using EMI technique is a very effective way of health monitoring in comparison to the traditional visual inspection method of health monitoring.
In this study a PZT-structure interaction was modelled using the commercially available finite element software ANSYS, version 13. The conductance signature was obtained for the undamaged beam. So when there will be any damage in the beam, the conductance signature of the beam will be different. By analysing the conductance signature of the damaged beam the location and extent of the damage can be found out.

CHAPTER 7

REFERENCES

[1] Bhalla, S.,**" A mechanical impedance approach for structural identification, health monitoring and non-destructive evaluation using piezo-impedance transducer"**, (2004), *PhD Thesis* Nanyang Technological University, Singapore

[2] Chhabra, D., Narwal, K. and Singh, P.,**" Design and Analysis of Piezoelectric Smart Beam for Active Vibration Control"**, (2012).

[3] Cho, S., Yun, C.B., Lynch, J.P., Zimmerman, A.T., Spencer Jr., B.F. and Nagayama, T., **"Smart Wireless Sensor Technology for Structural Health Monitoring of Civil Structures"**, (2008), Steel Structures 8 (2008) 267-275

[4] Claus-Peter Fritzen, **"Vibration-based Structural Health Monitoring – Concepts and Applications"**, (2005 Sep 15), *Trans Tech Publications, Switzerland*, Vols. 293-294, pp 3-20

[5] Duan, W.H., Wang, Q. and Quek, S.T.,**" Applications of Piezoelectric Materials in Structural Health Monitoring and Repair: Selected Research Examples"**, (2010).

[6] Fairweather, J. A., **"Designing with active materials: an impedance based approach"**, (1998), *PhD Thesis* Rensselaer Polytechnic Institute, New York

[7] Giurgiutiu, V.,**" Structural health monitoring with piezoelectric wafer active sensors – predictive modelling and simulation"**, (2007), *INCAS Bulletin*, Vol. 2, No. 3, 2010, pp. 31-44, Sept. 2010.

[8] Hong, K., Lee, J., Choi, S.W., Kim, Y. and Park, H.S.,**" A Strain-Based Load Identification Model for Beams in Building Structures"**, (2013).

[9] Hu, X., Zhu, H. and Wang, D.,**" A Study of Concrete Slab Damage Detection Based on the Electromechanical Impedance Method"**, (2014).

[10] Lalande, F., **"Modelling of the induced strain actuation of shell structures"**, (1995), *PhD Dissertation*, Virginia Polytechnic Institute and State University, Blacksburg, VA

[11] Liang, C., Sun, F. P. and Rogers, C. A., **"Electro-mechanical impedance modelling of active material systems"**, (1996), *Smart Mater. Struct.* **5** 171–86

[12] Parameswaran, A.P., Pai, A.B., Tripathi, P.K. and Gangadharan, K.V.,**" Active Vibration Control of a Smart Cantilever Beam on General Purpose Operating System"**, (2013).

[13] Peairs, D.M.,**" High Frequency Modelling and Experimental Analysis for Implementation of Impedance-based Structural Health Monitoring"**, (2006).

[14] Peng, D.,**" Study on the Mechanical Characteristics of Steel Fiber Reinforced Concrete Crack using Strain Gauges for Structure Health Monitoring"**, (2012).

[15] Yang, Y., Hu, Y. and Lu, Y.,**" Sensitivity of PZT Impedance Sensors for Damage Detection of Concrete Structures"**, (2008).

[16] Yang, Y., Lim, Y.Y. and Soh, C.K.,**" Practical issues related to the application of the electromechanical impedance technique in the structural health monitoring of civil structures: II. Numerical verification"**, (2008), Smart Materials and Structures Volume 17 Number 3.

[17] Yang, Y. and Miao, A.,**" Effect of External Vibration on PZT Impedance Signature"**, (2008).

[18] Yao, J. T. P. , Natke, H.G., **"Damage detection and reliability evaluation of existing structures"**, (1985), Structural Safety, Volume 15, Issues 1-2.August 1994,Pages 3-16

[19] Zhang, Y., Xu, F., Chen, J., Wu, C. and Wen, D.,**" Electromechanical Impedance Response of a Cracked Timoshenko Beam"**, (2011).

[20] Zhou, S., Liang, C. and Rogers, C. A., **"Integration and design of piezoceramic elements in intelligent structures"**, (1995), *J. Intell. Mater. Syst. Struct.* **6** 733–43